

IMPACT MODELING OF VISCOELASTIC SYSTEMS

A THESIS

Presented to

The Faculty of the Division of Graduate
Studies and Research

By
Mangharjansah
K. Rao

In Partial Fulfillment

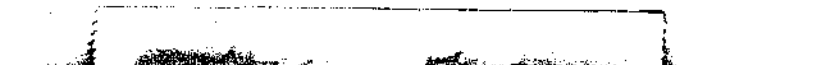


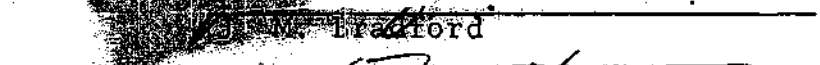
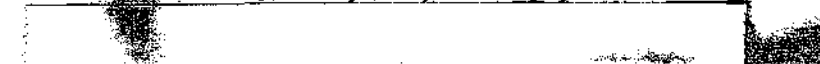

of the Requirements for the Degree
Master of Science in Mechanical Engineering

Georgia Institute of Technology

November, 1973

IMPACT MODELING OF VISCOELASTIC SYSTEMS

Approved:

W. D. Freeston

Date approved by Chairman: 12-11-1973

ACKNOWLEDGMENTS

I wish to express my sincere appreciation to my advisor, Dr. Wolfgang Wulff, for suggesting the topic of this research. I am indebted to him for his guidance, encouragement and help during all stages of this research. I would also like to thank Dr. W. D. Freeston and Dr. J. M. Bradford for their valuable suggestions and careful review of the manuscript.

Finally, I wish to acknowledge the support of the National Bureau of Standards in connection with this research.

TABLE OF CONTENTS

	Page
ACKNOWLEDGMENTS.	ii
LIST OF FIGURES.	v
NOMENCLATURE	vii
SUMMARY.	ix
Chapter	
I. INTRODUCTION.	1
Relevance of the Problem	
Present State of the Art	
Advances Required	
Present Investigation	
II. IMPACT MODELING ANALYSIS.	12
Problem Formulation	
Model Description	
Governing Equations	
Scaling Parameters	
Solution	
III. SIMPLIFIED ANALYSIS OF LINEAR MATERIAL RESPONSE	27
Force History	
Corresponding Deformation	
Instant of Maximum Deformation	
Parameter Constraints	
Energy Absorption	
IV. RESULTS	43
Graphical Presentation	
V. DISCUSSION.	62
VI. CONCLUSIONS AND RECOMMENDATIONS	67

Page

APPENDICES

A. AN EQUIVALENT MODEL TO ONE SHOWN IN FIGURE 1. . . 70

B. DERIVATION OF EQUATION 2.11 73

C. DETAILS OF NORMALIZATION. 76

D. SYSTEM PARAMETERS IN TERMS OF NONDIMENSIONAL
PARAMETERS. 82

BIBLIOGRAPHY 86

LIST OF FIGURES

Figure	Page
1. Schematic of Impact System.	15
2. Stress-Strain Characteristic of Four Parameter Padding System.	18
3. Analogue Computer Circuit Diagram	26
4. Graphical Solution to Equation 3.39	35
5. Padding Deformation History During Impact, Effect of Parameter a	46
6. Padding Deformation History During Impact, Effect of Parameter b	47
7. Padding Deformation History During Impact, Effect of Parameter c	48
8. Padding Deformation History During Impact, Effect of Parameter d	49
9. Impact Force as a Function of Time with a as a Parameter	50
10. Impact Force as a Function of Time with b as a Parameter	51
11. Impact Force as a Function of Time with c as a Parameter	52
12. Impact Force as a Function of Time with d as a Parameter	53
13. Stress-Strain Response as a Function of Parameter a	54
14. Stress-Strain Response as a Function of Parameter b	55
15. Stress-Strain Response as a Function of Parameter c	56
16. Stress-Strain Response as a Function of Parameter d	57

Figure		Page
17.	Energy Absorption with a as Parameter.	58
18.	Energy Absorption with b as Parameter.	59
19.	Energy Absorption with c as Parameter.	60
20.	Energy Absorption with d as Parameter.	61
21.	An Equivalent Model to One Shown in Figure 1 . .	71

NOMENCLATURE

A	Impacting object parameter, defined by Equation 2.27
a	Acceleration, deceleration in Equation 1.1
a	Padding parameter, defined by 2.29
B	Impacting object parameter, defined by Equation 2.28
b	Padding parameter, defined by Equation 2.30
C	Viscous damping coefficient
c	Padding parameter, defined by Equation 2.31
d	Padding parameter, defined by Equation 2.32
E	Kinetic impact energy
e	Padding parameter, defined by Equation 2.33
$E_1(V, \epsilon)$	Rate and strain dependent modulus
$E_1(V)$	Rate dependent modulus
F	Force
g	Gravitational acceleration
K	Spring constant
m	Mass of the impacting object
n	Exponent in Equation 1.1
$P_1 \dots P_4$	Independent padding parameters, Equations 2.37, 2.38, 2.39, 2.40
SI	Severity index, Equation 1.1
EDI	Equivalent displacement index
V_0	Impactor velocity
W	Absorbed energy, Equation 3.56

x	Displacement
y	Total padding deformation, Equation 2.4
α	Normalized damping support parameter, Equation 2.34
β	Normalized damping support parameter, Equation 2.35
γ	Normalized inertia support parameter, Equation 2.36
δ	Padding thickness
ϵ_1	Partial padding deformation due to the Kelvin element
ϵ_2	Partial padding deformation due to the spring with constant K_2
ϵ_3	Partial padding deformation due to the dash pot with constant C_2
ζ	Normalized impacting object displacement, Equation 2.17
η	Normalized support displacement, Equation 2.18
ξ	Normalized total padding deformation, Equation 2.16
τ	Time
τ^*	Normalized time, Equation 2.15
ϕ	Normalized force, Equation 2.19
ω	Normalized absorbed energy, Equation 3.57

Subscripts

i	initial, start of impact
f	final, end of impact
max	maximum
o	initial and reference

Superscript

dot	differentiation with respect to time
-----	--------------------------------------

SUMMARY

Impact injuries of varying intensities are frequently encountered by certain professional groups such as miners, construction workers, firemen, policemen, and by participants in some sports events like football, fencing and hockey. Even though protective clothing (i.e., uniforms) consisting of padding materials, etc., have been designed for a few of the above categories (viz., contact sports) there exists no systematic method to select protective clothing based on such scientific considerations as the ability to reduce stress concentrations and absorb and dissipate kinetic energy.

Consequently, an impact modeling analysis is presented to help in the selection of optimum protective padding (clothing) systems, for the purpose of mitigating impact injuries. The analysis aims at predicting padding performance by identifying relevant padding and process parameters.

An analogue computer solution is presented to predict impact response of protective clothing systems in terms of strain versus time, stress versus time, stress versus strain, and energy absorption versus time, during the period of impact.

Scaling parameters are developed from the equations of motion. Analytical expressions for deformation, for time

of maximum deformation, and for absorbed energy during impact are developed.

CHAPTER I

INTRODUCTION

Relevance of the Problem

The major portion of more than 50 million injuries suffered annually in the United States can be broadly classified as impact injuries. In 1959, the United Nations recorded [1]^{*} nearly 12,000 deaths in one year among the motor-cycling population of the countries of Western Europe alone. Almost all of them were impact type injuries. Seventy per cent of them were head injuries and 58 per cent of all injuries resulting in death involved fracture of the skull. Almost all of the injuries and accidental deaths occurring in automobile accidents are the result of impact type injuries only. Certain occupational groups such as miners, policemen, firemen, construction workers, and participants in certain sports activities such as fencing, football, and hockey, are prone to receive impact injuries of varying intensities resulting in bone fractures, dislocations, ruptures, contrusions and in some extreme cases even death.

Impact injuries result when a flying or falling object hits a victim, or when the victim itself hits some

^{*}Numbers in brackets refer to the Bibliography.

object while falling down from its initial level to the same level or to a different level. Common to all impact injuries, however, is the development of a strain field within all or parts of a victim's body. The character of injury depends upon the extent of the field, the magnitude of the strain, and the time rate of strain development. Permanent tissue damage results from irreversible, non-elastic strains and is associated with the dissipation of kinetic energy within the tissue.

It has been recognized that the severity of the injury can be greatly reduced by protective clothing. Consequently, protective clothing in the form of flexible paddings and combinations of such paddings with semi-rigid shells have been developed for a few occupational groups, such as football and hockey players, race car drivers and cyclists. Even though it has been generally recognized that the protective clothing must function to reduce the strain, the strain rate and the kinetic energy entering the body, there exists no systematic method to assess accordingly the effectiveness of protective clothing (padding) systems.

Present State of the Art

The objective of the present endeavor is to help in establishing conclusively the relative protective capabilities of given padding systems, which are primarily made of fibrous materials, plastics, metals and combinations thereof.

Consequently a brief description of the padding systems, of the information concerning the testing methods used to grade materials for impact protection and of the body response to impact are given below.

Padding Systems

The main properties of protective padding systems used for reducing the severity of impact injuries are: (1) they should not be penetrated by the impacting object, (2) they must be able to spread load over a large area so as to reduce local stress concentration, and (3) they must be able to dissipate some of the kinetic energy of impact.

Ideally the above goals can be achieved by means of a rigid outer layer designed to distribute impact pressure, backed by an energy absorbing padding. However, the use of such type of material to protect all the vital parts of the body areas, not only causes much discomfort to the wearer, but also reduces his mobility to such an extent that occupational duties can not be satisfactorily carried out. Consequently, the actual protective equipment used is a reasonable compromise between the amount of protection required on one hand and comfort and mobility considerations on the other. Because of the above reason, the protective clothing for persons who must be active and agile is usually comprised of combinations of flexible, semi-rigid, and rigid protective paddings. The most vulnerable portions of the body are protected by rigid padding, i.e., head, toes, knees,

elbows, shoulders. Because of mobility considerations, flexible paddings must be used to protect the body trunk. The outer layer of flexible padding assemblies is usually a densely woven fabric in order to prevent penetration by the impacting object. This layer also helps to spread load over a large area and thus helps in reducing stress concentration effects.

The outer layers of better, light-weight rigid protective materials, e.g. helmets, are usually of a fiber reinforced resin matrix. The rigid outer layer is usually backed by an energy absorbing layer. At the present time, polystyrene foam molded from expandable beads is commonly used. Needled felt and other types of non-woven fiber assemblies are also used as the energy absorbing layers [18]. The performance of such assemblies on a weight basis increases with decreasing volumetric density. However, mobility considerations limit the tolerable thickness.

Testing Methods

Considerable amount of data is available on testing methods and performance of single fibers at various strain rates up to 10,000 per cent/second [4,5,7,8,9,10].

The tensile properties of fibers have been determined over a broad range of conditions. Fabric Research Laboratories has developed a piston type tensile tester for testing fibers and yarns at jaw speeds of 40 to 100 feet per second and temperatures to 400°F. They also developed a ballistic

type of tensile tester for impacting fabrics and webbings at missile speeds of 150 to 750 feet per second [7,8]. Testing equipment has been constructed for measuring the tensile properties of textile structures with strengths to 1000 pounds at air temperatures to 2000°F and at jaw speeds of 50 to 200 feet per second [9], to fill the gap in testing capabilities between the above two testers. All the above three testing machines are mainly research tools. At present, data is available on a series of materials at strain rates up to around 10000 per cent per second. But, the performance of the padding materials which are random assemblies of the fibers can not be completely judged from the performance of fibers. From the literature survey it is observed that very little data is available on the impact performance of padding materials.

The impact resistance of some rigid shell materials has been evaluated by the drop ball method. Helmets for occupants of vehicles are tested for impact attenuation and penetration under carefully specified conditions as described in the American National Standards (ANSI 90.1 - 1971) "Specifications for Protective Head Gear for Vehicular Users."

The ballistic impact resistance of various candidate shell materials has also been evaluated under U. S. Government Defense Contracts. However most of the test procedures and test data are classified.

The U. S. Army Natick Laboratories built test

equipment to test energy absorbing materials. Their main interest was in energy absorbing materials to be placed under heavy equipment being air dropped. The test equipment consists of two platforms whose weight can be varied and mounted on a thirty feet long track. The platforms were propelled pneumatically and impacted at the center. The energy absorbing material to be evaluated was mounted on the front of one of the platforms. Appropriate instrumentation permitted the energy absorbed to be measured.

Some of the commercially available testing equipment which can be used in the impact testing of padding materials in their end use condition or with slight modifications is described below.

Monterey Research Laboratories, Inc., Monterey, California, manufactures general purpose shock testing machines called Impac 66 Mark II, and Impac 99 Mark II, which are designed for a wide range of shock tests. With minor modifications these machines can be used for impact testing also.

Monterey Research Laboratories, Inc., also manufactures a special machine called Impac 15-HF which is specially designed for the impact testing of padding materials. A 15 pound head form drop weight with a 6.5 inch diameter hemisphere as specified in SAE J 921 is made to fall vertically down in free fall along guide rails. It impacts padding material placed on the reaction mass. Maximum

allowable acceleration of 1000 g and maximum impact velocities of 22 feet per second can be achieved. By means of accelerometers, mounted on the dropping head form, and a dual trace oscilloscope the acceleration profile can be easily obtained. The machine can easily be modified to widen its range of applications.

Body Responses

In order to protect the human body from impact injury (by means of protective padding systems) it is necessary to know the susceptibility of the human body to impact injury and the response of the human body to impact.

Any reference to the susceptibility of the body to impact must involve the description of the specific type of impacting structure, the impact site and the nature of the impact. The geometry and the mechanical properties of the impacting object and the rate of load application are extremely important parameters. The relative velocities and masses are significant but in order to completely isolate all injury producing effects, the description of body motion must be supplied.

The best demonstration of the above fact comes from the study of the relative effectiveness of football helmets, mainly done at Wayne State University. It was quite conclusively demonstrated that when a stationary head is impacted the damage done to the brain structure is quite different from that caused by a fall of the head. The latter case

causes high negative pressures in cerebral fluid which cause severe brain damage that is not produced in the first case.

Therefore, it is necessary to identify the cases where the injury causing impact occurs while the body is stationary or in motion and to determine the velocity, acceleration and the mass of the impacting body at the time of impact. Another important point to be noted in discussing the susceptibility of body injury is that any specific impact will have a variety of effects depending on which part of the body is involved.

The response of the body to impact can be represented by its peak deceleration, its average deceleration, the severity index (SI), the effective displacement index (EDI), and the available clinical description of the injury. Where the severity index is defined as

$$SI = \int_{\tau_i}^{\tau_f} (a/g)^n dt \quad (1.1)$$

and has the dimensions of time. In the above equation, τ_i and τ_f stand for initial and final times of impact, respectively, 'a' stands for acceleration of the body, 'g' stands for acceleration due to gravity, and 't' for time. The exponent 'n' was derived by Gadd [2] to have a value of 2.5.

The equivalent displacement index (EDI) of Brinn and

Staffeld [3] equals the displacement from the equilibrium position of a viscoelastic Maxwellian system which simulates the body part of interest.

Advances Required

A brief discussion of some of the important factors and variables to be considered in the testing and evaluation of padding materials is presented below.

Very little information is available in the literature on the performance of fiber reinforced composites or flexible fiber assemblies in impact protection applications. The problem is particularly difficult to analyze because of multiple strain wave reflections that take place in fiber assemblies. The velocity of strain wave propagation and multiple strain wave reflections in the yarn crossover intersections in the fibrous padding materials at high impact rates must be considered in choosing the test specimen size [4,5].

The compression energy absorption of foams and fiber assemblies can be obtained quasi-statically with an Instron. However such data is not of much use in designing protective paddings. The candidate materials are strain rate sensitive with different materials being effected to different degrees. Polymeric foams, which are extensively used as impact energy absorbing materials, are a good example of the above fact. The material properties of the polymeric foams are functions

of both strain and strain rate. For such materials the rate and strain dependent modulus $E(v, \epsilon)$ can be represented by the product of two functions, one $E_1(v)$ depending on the rate of deformation only and the other depending on the strain only [6].

The load deformation response of polymeric materials both plastics and fibers vary significantly with temperature and the fiber moisture content, i.e., the humidity of the environment. Generally, the fiber strength increases, elongation decreases and the energy absorption decreases with decreasing temperatures and decreasing humidity. Therefore, in the experimental evaluation of some of the padding materials, these parameters must be carefully controlled.

Presently several researchers are working on the impact response of fiber assemblies. Efforts are now being made to solve equations based on a continuum approach [10]. The effects of fiber friction at fiber crossovers as well as layers of backing fibers are being included. Because of the complexity of the fiber assemblies, it is not expected that the above analysis will accurately model the quantitative response of the fiber assemblies. However, it should indicate the relative significance of various parameters, guide the test method design and further the analysis of the test data. Consequently for the foreseeable future, in order to determine the relative merits of various candidate

padding materials, it will be necessary to evaluate them experimentally, using the test equipment that simulates as closely as possible the end use environment.

Present Investigation

In the following chapters an impact modeling analysis will be performed with a view towards deriving suitable scaling laws. The analysis will be based on simplified differential equations of motion with subsequent dimensionless analysis. Mainly because of the complexity of padding description, the following analysis can not be complete, nevertheless broad trends of padding behavior will be obtained. The main objective of the modeling analysis is to help in rating protective padding materials in accordance with their relative abilities to protect from impact injuries.

Briefly, the modeling analysis serves to characterize padding systems, to evolve scaling parameters, to develop test procedures by which to compute the impact energy absorption from suitable sensor signals and to indicate response trends of padding systems.

CHAPTER II

IMPACT MODELING ANALYSIS

Problem Formulation

The purpose of the impact modeling analysis is:

- (1) to predict the response of the protective padding systems to impact under a wide range of impact parameters and for a wide range of body responses from a minimum possible set of experimental data,
- (2) to prescribe the most desirable padding properties for specific impact situations, and
- (3) to develop procedures (within the limitations of simplifying assumptions) or organize and interpret experimental data and also to determine approximate values of parameters that can not be measured directly.

The prediction of impact response is attempted through normalization of the appropriate equations of motion. This normalization yields the scaling parameters which serve to conclude from experimental data correlations to actual impact situations. The equations of motion can be solved, either through analogies or numerical techniques, to yield the energy absorption by the padding in terms of its system parameters and of the impact parameters. Analytical results obtained from the integration of the equations of motion are

used to select optimum padding properties.

The system consists of three parts, the impactor, the padding and the impacted object. The human body or parts of it may assume the roles of either the impactor (falling body) or the impacted object (stricken body).

All three components generally are capable of elastic energy storage and of energy dissipation. Depending on the required accuracy and on the computational complexity accepted, each component may be subdivided into a number of discrete subsystems. Each subsystem can be represented by three parameters, the subsystem's mass, m , spring constant, K , and damping coefficient, C . The subsystems may be coupled, either in series or in parallel, through the constraints of force continuity, $\Sigma F=0$, and of displacement continuity, $\Sigma x=0$.

The analysis presented here describes the interactions of a stiff impactor without energy storage or dissipation, a four-parameter padding system and a visco-elastic impactee representing the support. The components are discussed in more detail below.

Model Description

The system discussed here simulates the impact situations where the padded body falls onto a rigid surface or where the padded body is stricken by a rigid object. The

system consists of three parts shown in Figure 1, which are described below.

Impactor

The impactor is taken to be rigid and to be completely specified by its mass m_1 and its vertical downward velocity \dot{x}_1 at the time $\tau=0$ at impact. The impactor is assumed to strike the protective padding system perpendicularly to their common interface. The equation of motion of the impactor is

$$m_1 \ddot{x}_1 = m_1 g - F_1 \quad (2.1)$$

where F_1 represents the force exerted by the fabric on the impactor and g stands for the gravitational acceleration. Superscripted dots designate differentiation with respect to real time τ . The origin of the coordinate system is chosen such that, at time $\tau=0$.

$$x_1(0) = 0, \quad \dot{x}_1(0) = V_0, \quad (2.2)$$

where V_0 is the impacting velocity.

Protective Padding

The elements of the model used for representing the protective padding materials consist of an equivalent mass m_2 . Generally m_2 is negligibly small when compared to m_1 . It also consists of a spring characterized by the spring

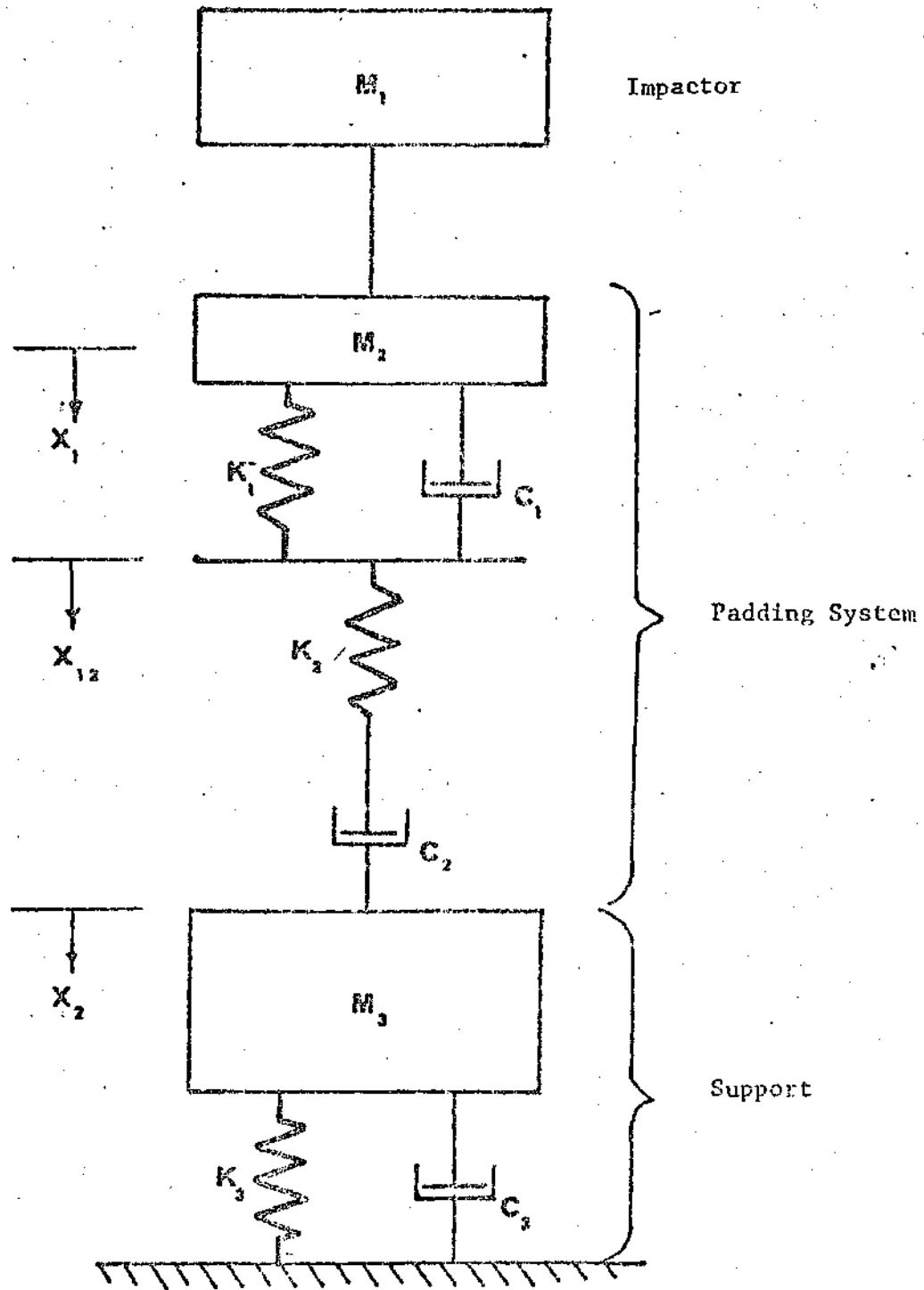


Figure 1. Schematic Of Impact System

with constant K_2 and a dash pot with constant C_2 connected in series (Maxwellian element). This Maxwellian element is connected in series to a spring with constant K_1 and dash pot with constant C_1 connected in parallel (Kelvin element). The four parameters of the above model are to be determined experimentally and are expected to depend on strain and on strain rate.

The visco-elastic padding system represented by this model has the creep characteristics of the polymers [11] and serves as a first approximation to simulate the response to impact of a fibrous material. The computed response of the model* is represented by linear differential equations with constant coefficients.

Under time-invariant force, F_2 , the spring with constant K_2 simulates the mechanism of elastic deformation which develops instantaneously and which is at any instant proportional to the magnitude of the applied force (in accordance with the Hooke's law) $\epsilon_2 = F_2/K_2$. The Kelvin element represents the mechanism of high elastic deformation of this model, the deformation will assume the limiting value of F_2/K_1 set by the spring constant K_1 of the spring. The rate of extension can be described by the time constant of the element viz., $\tau_k = C_1/K_1$. Finally the dash pot with constant C_2 represents the mechanism of plastic deformation

* An equivalent model, which has almost the same computed response as the above model and which is advantageous under certain conditions, is given in Appendix A.

which is irreversible (Figure 2).

The deformation $x_1 - x_2$ as a function of time under the general force $F_2(\tau)$ is obtained by dividing the deformation up into three parts: ϵ_1 for the deformation of the spring with constant K_1 , connected in parallel to the dash pot with coefficient C_1 , ϵ_2 for the deformation of the spring with constant K_2 , and ϵ_3 for the deformation of the dash pot with coefficient C_2 . Then

$$x_1 - x_2 = \epsilon_1 + \epsilon_2 + \epsilon_3 = y \quad (2.4)$$

The force increment dF_2 acting on the system produces in its upper portion the deformation $d\epsilon_1$ with the reactions $K_1 d\epsilon_1 + C_1 \dot{\epsilon}_1 d\tau$. Therefore

$$\dot{F}_2 = K_1 \dot{\epsilon}_1 + C_1 \ddot{\epsilon}_1 \quad (2.5)$$

The position $\epsilon_1=0$ is chosen such that the weight m_2g is supported by the springs with constants K_1 and K_2 . Any force increment dF_2 deforms the spring with spring constant K_2 by $d\epsilon_2 = dF_2/K_2$. From this follows

$$\dot{F}_2 = K_2 \dot{\epsilon}_2 \quad (2.6)$$

The lower dash pot with damping coefficient C_2 yields proportionally to the force F_2 , the reciprocal $1/C_2$ and the

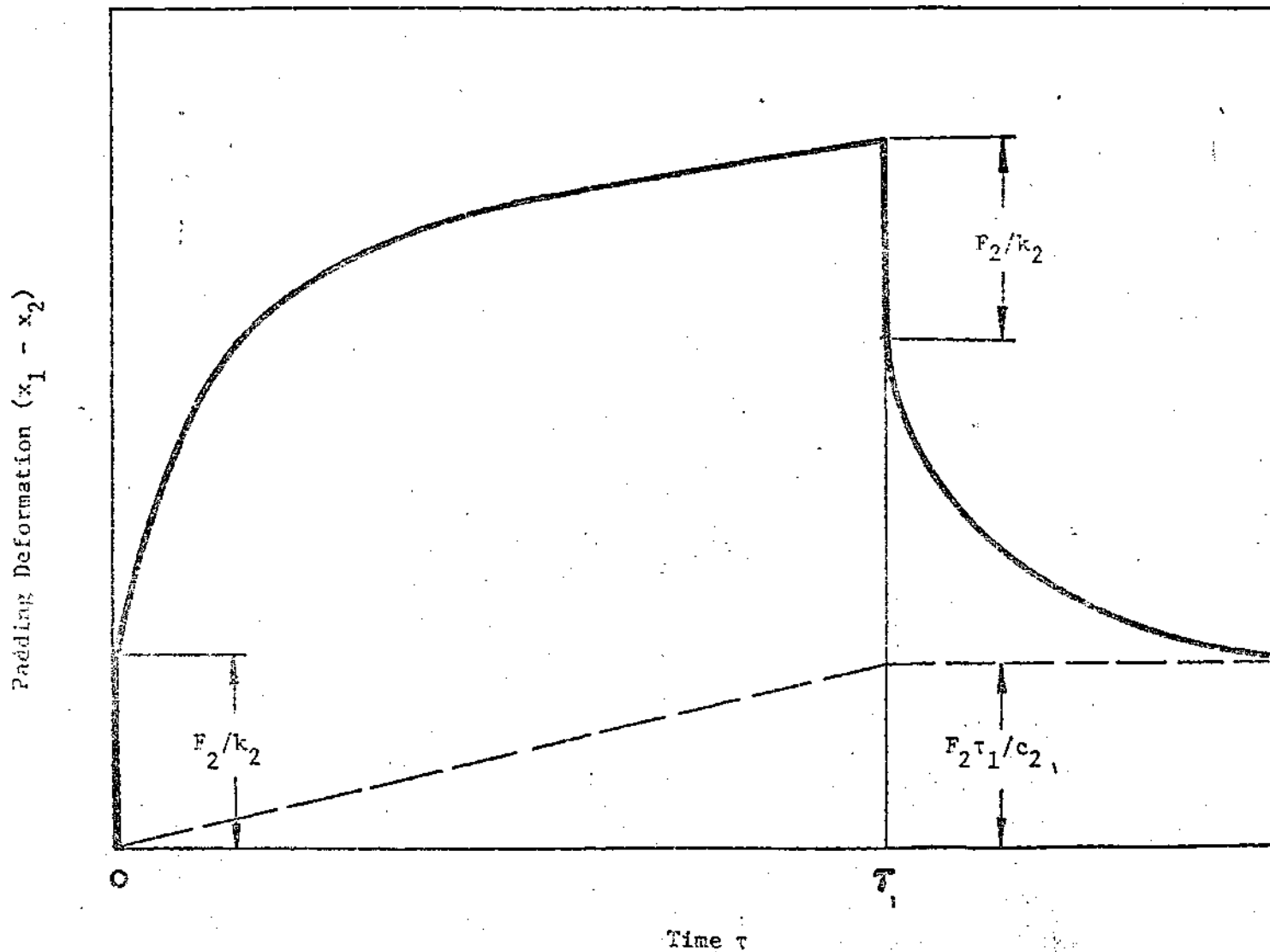


Figure 2. Stress-Strain Characteristic of Four Parameter Padding System

time increment $d\tau$, or

$$F_2 = C_2 \dot{\epsilon}_3 \quad (2.7)$$

The motion of the equivalent mass m_2 under the actions of the forces F_1 and F_2 , exerted by the sled and the four-element viscoelastic simulator respectively, is given by

$$m_2 \ddot{x}_1 = F_1 - F_2 \quad (2.8)$$

This completes the description of the padding response to both the impacting object and the padding support.

Support

The impacted object serves as padding support. It is described in terms of its inertia, its elasticity and its viscous dissipation, namely the mass m_3 , the spring constant K_3 and the damping coefficient C_3 . After choosing the origin $x_2 = 0$ such that the weights $(m_2 + m_3)g$ are supported by the lowest spring with constant K_3 one obtains for motion of the support.

$$m_3 \ddot{x}_2 = F_2 - K_3 x_2 - C_3 \dot{x}_2 \quad (2.9)$$

The parameters m_3 , K_3 , C_3 must be selected to represent the object which absorbs the impact.

Governing Equations

The deformation history, the variation of force with time and the absorbed impact energy can be computed from the equations of motion and the initial conditions.

Equations of Motion

Adding equations 2.1 and 2.8 eliminates the force F_1

$$\ddot{x}_1 = (m_1 g - F_2) / (m_1 + m_2) \quad (2.20)$$

From equation 2.9 follows

$$\ddot{x}_2 = (F_2 - K_3 x_2 - C_3 \dot{x}_2) / m_3 \quad (2.11)$$

The net deformation of the padding is defined by equation 2.4. From this definition and equations 2.5, 2.6, 2.7 and 2.8, it follows that

$$K_1 \dot{y} + C_1 \ddot{y} = K_1 \sum_{i=1}^3 \dot{\epsilon}_i + C_1 \sum_{i=1}^3 \ddot{\epsilon}_i$$

or

$$\ddot{F}_2 = -K_1 K_2 F_2 / (C_1 C_2) - \frac{K_2}{C_1} \left(1 + \frac{K_1}{K_2} + \frac{C_1}{C_2}\right) \dot{F}_2 + \frac{K_1 K_2 \dot{y}}{C_1} + K_2 \ddot{y}^* \quad (2.12)$$

Equations 2.10, 2.11, and 2.12 are the three differential equations for the dependent variables x_1 , x_2 and F_2 .

* Derivation of this equation is given in Appendix B.

Initial Conditions

The system is initially at rest everywhere except at the interface between impacting object and the padding. Thus, as $\tau=0$

$$x_1 = x_2 = \dot{x}_2 = 0 \quad (2.13)$$

$$y = 0 \quad (2.14)$$

$$\dot{x}_1 = V_0 \quad (2.15)$$

Here V_0 represents the impacting velocity.

Scaling Parameters

The modeling rules are necessary to generalize the results of the analysis and to relate laboratory tests to real-life impacts. The equations of motion and initial conditions are normalized to derive the modeling rules. To make possible an order of magnitude comparison between the terms in the equation of motion and thereby between the concurrent processes, the equations are normalized such that the nondimensional independent and the relevant dependent variables, together with the necessary derivatives are of order unity.

Introducing the nondimensional

time	$\tau^* = \tau V_0 / \delta$	(2.15)
------	------------------------------	--------

deformation	$\xi = y / \delta = \zeta - \eta$	(2.16)
-------------	-----------------------------------	--------

sled motion	$\zeta = x_1 / \delta$	(2.17)
-------------	------------------------	--------

support motion	$\eta = x_2 / \delta$	(2.18)
----------------	-----------------------	--------

contact force $\phi = F_2 \delta / (m_1 V_0^2)$. (2.19)

The following three equations replace equations 2.10, 2.11, and 2.12, respectively:

$$\zeta'' = A - B\phi^* \quad (2.20)$$

$$\eta'' = -\alpha\eta' - \beta\eta + \gamma\phi \quad (2.21)$$

$$\phi'' = -a\phi' - b\phi + c\xi'' + d\xi' \quad (2.22)$$

Where primes designate differentiation with respect to τ^* .

The initial conditions are derived from equations 2.2, 2.13, and 2.14:

at $\tau^* = 0$ $\zeta' = \xi' = 1$ (2.23)

$$\phi = \zeta = \eta = \eta' = 0 \quad (2.24)$$

$$\xi = 0 \quad (2.25)$$

$$\phi' = e \quad (2.26)$$

The ten nondimensional groups in equations 2.20, 2.21, and 2.22, are:

*The derivation of these equations and necessary initial conditions in nondimensional terms is given in Appendix C.

the sled characteristics

$$A = Bg\delta/V_o^2 \quad (2.27)$$

$$B = \frac{m_1}{m_1+m_2} \approx 1, \quad (2.28)$$

the padding characteristics

$$a = (1+p_1+p_2)p_3/p_1 \quad (2.29)$$

$$b = p_2p_3^2/p_1 \quad (2.30)$$

$$c = p_3/p_4 \quad (2.31)$$

$$d = b/p_4 \quad (2.32)$$

$$e = p_3/p_4 \quad (2.33)$$

and the support characteristics

$$\alpha = (\delta/V_o)C_3/m_3 \quad (2.34)$$

$$\beta = (\delta/V_o)^2K_3/m_3 \quad (2.35)$$

$$\gamma = m_1/m_2 \quad (2.36)$$

The five padding characteristics a , b , c , d , and e are expressed in terms of four independent padding scaling parameters:

$$p_1 = C_1/C_2 \quad (2.37)$$

$$p_2 = K_1/K_2 \quad (2.38)$$

$$p_3 = (K_2 \delta)/(C_2 V_0) \quad (2.39)$$

$$p_4 = (m_1 V_0)/(C_2 \delta) \quad (2.40)$$

The normalization of equations 2.2, 2.10, 2.11, 2.12, 2.13, and 2.14 has led to the reduction of padding and process parameters from twelve to nine. This reduction was to be expected from the Pi-theorem and the fact that there are three fundamental dimensions involved: time, length and mass. The nine scaling groups A, B, P_1, \dots ; α , β , and γ are not unique, in that there can be formed new such groups by any combination of the groups presented above. The minimum number of scaling parameters, however, required for complete scaling of the chosen impact model is nine.

Complete modeling requires that all the nine scaling parameters be the same in the laboratory experiment as in the actual impact to be simulated. However, some of the parameters may be small enough that the associated terms in the governing equations can be ignored, and partial modeling adequately describes the impact. As an example one may ignore gravity when the impact velocity is sufficiently large, or, more specifically when

$$V_0^2 \gg (m_1 + m_2)/m_1 g \delta$$

then the parameter A approaches zero. Which of the parameters are the most dominant ones needs to be determined for specific padding properties separately.

Solution

The set of ordinary second order differential equations, 2.20 through 2.22, subject to the initial conditions in equations 2.23 through 2.26, was solved with the aid of an analogue computer. A Systron-Donner Model 10/20 analogue computer with a Hewlett-Packard multitrace oscilloscope and a kdp14 Moseley 7005 B-key recorder (Hewlett-Packard) were used. The Model 10/20 is an all solid state analogue computer with an operating range of ± 100 V and expansion capabilities for up to 24 operational amplifiers. This computer has computing resistor and capacitor networks with a 0.01% accuracy, a panel voltmeter having a null mode of measurement with 0.02 per cent of full scale resolution. The analogue computer circuit diagram is shown in Figure 3. The results are presented in Chapter IV.

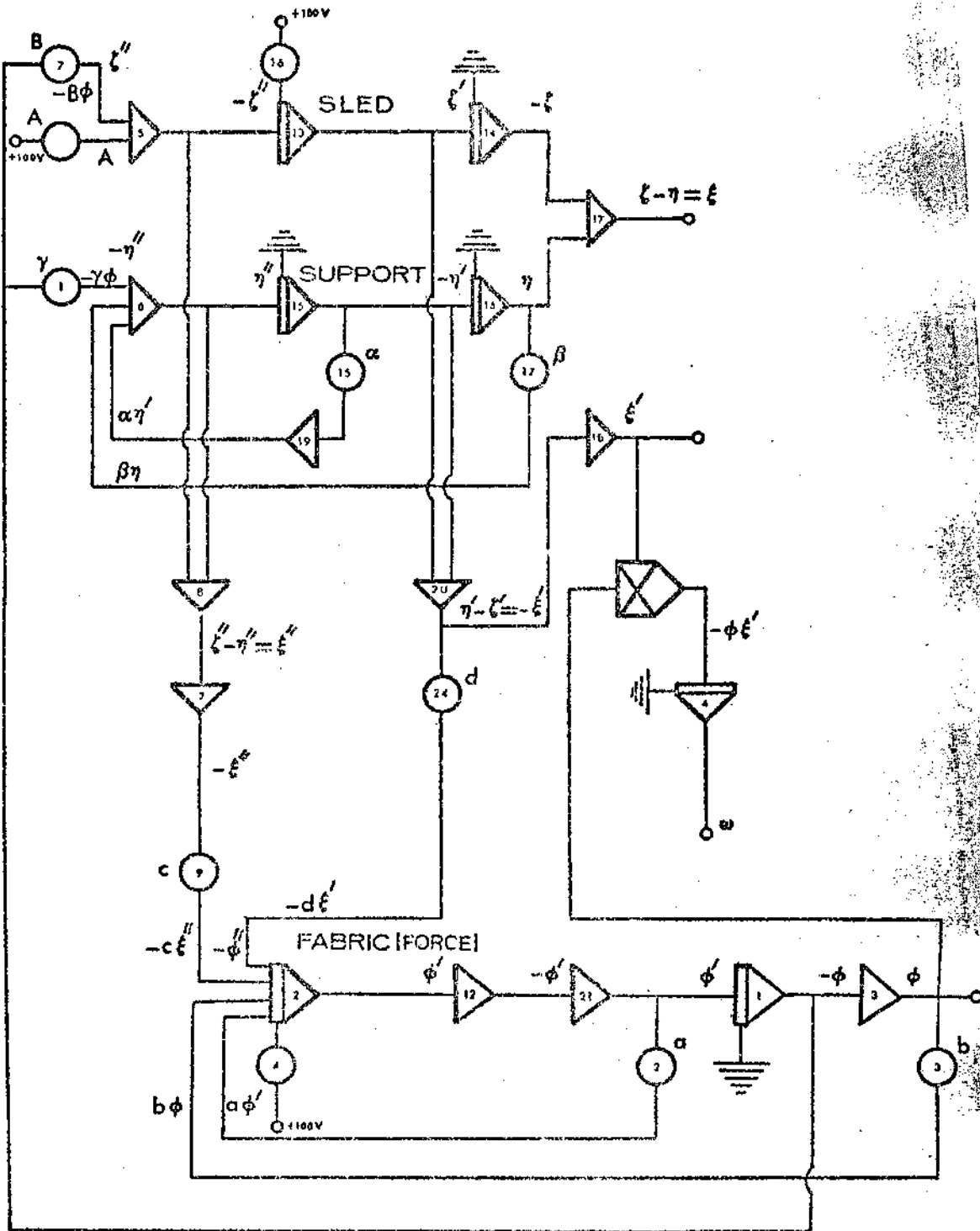


Figure 3. Analogue Computer Circuit Diagram

CHAPTER III

SIMPLIFIED ANALYSIS OF LINEAR MATERIAL RESPONSE

For the purpose of finding the constraints on the parameters (a, b, c, and d) such that the maximum normalized deformations ξ_{\max} is less than or equal to one, a simplified analysis of linear material response is presented below. This consists of an expression for normalized deformation ξ as a function of normalized time τ^* , a method of finding the instant of maximum deformation, and an expression for the normalized energy absorption ϕ as a function of normalized time τ^* .

Force History

From the shape of the analogue solution of nondimensional force vs. nondimensional time curves, it can be seen that ϕ can be represented by a function of the form $A\tau^* e^{-m\tau^*}$ where A and m are the constants to be determined by curve fitting techniques.

Corresponding Deformation

From equation 2.22, rearranging,

$$c\xi'' + d\xi' = \phi'' + a\phi' + b\phi. \quad (3.1)$$

Differentiating $\phi = A\tau^*e^{-m\tau^*}$ with respect to τ^* yields first

$$\phi' = Ae^{-m\tau^*}[1-\tau^*m] . \quad (3.2)$$

Then

$$\phi'' = Ae^{-m\tau^*}(m^2\tau^*-2m) . \quad (3.3)$$

Substituting these values of ϕ , ϕ' , and ϕ'' in equation 3.1 and simplifying,

$$\xi'' + \frac{d}{c}\xi' = \frac{A}{c}e^{-m\tau^*}[\tau^*(m^2-am+b) + (a-2m)] . \quad (3.4)$$

Let,

$$c\rho = \frac{A}{c}[(m^2-am+b)] , \quad (3.5)$$

$$\sigma = \frac{A}{c}[a-2m] \quad (3.6)$$

and

$$v = d/c . \quad (3.7)$$

Then equation 3.4 becomes

$$\xi'' + v\xi' = \rho\tau^*e^{-m\tau^*} + \sigma e^{-m\tau^*} . \quad (3.8)$$

This is a second order, linear, nonhomogeneous differential equation with constant coefficients.

The general solution of the corresponding homogeneous equation is

$$\xi_n = L_1 + L_2 e^{-v\tau^*}, \quad (3.9)$$

where L_1 and L_2 are constants to be determined from the initial conditions.

Applying the method of undetermined coefficients to find the particular solution, let

$$\xi_p = R_1 \tau^* e^{-m\tau^*} + R_2 e^{-m\tau^*}. \quad (3.10)$$

Differentiating with respect to τ^* ,

$$\xi_p' = -R_1 m \tau^* e^{-m\tau^*} + (R_1 - R_2 m) e^{-m\tau^*}. \quad (3.11)$$

Again differentiating with respect to τ^* ,

$$\xi_p'' = R_1 m^2 \tau^* e^{-m\tau^*} + [R_2 m^2 - 2R_1 m] e^{-m\tau^*}. \quad (3.12)$$

Substituting these values of ξ_p' and ξ_p'' in equation 3.8,

$$\begin{aligned} R_1 m^2 \tau^* e^{-m\tau^*} + [R_2 m^2 - 2R_1 m] e^{-m\tau^*} + v[-R_1 m \tau^* e^{-m\tau^*} \\ + (R_1 - R_2 m) e^{-m\tau^*}] = p \tau^* e^{-m\tau^*} + \sigma e^{-m\tau^*}. \end{aligned}$$

Rearranging the above expression,

$$\begin{aligned} \tau^* e^{-m\tau^*} [R_1 m^2 - \nu R_1 m] + e^{-m\tau^*} [(R_2 m^2 - 2R_1 m) + \\ \nu(R_1 - R_2 m)] = \rho \tau^* e^{-m\tau^*} + \sigma e^{-m\tau^*} . \end{aligned} \quad (3.13)$$

Equating the coefficients of $\tau^* e^{-m\tau^*}$ and $e^{-m\tau^*}$ terms on the both sides of equation 3.13,

$$R_1 m^2 - \nu R_1 m = \rho \quad (3.14)$$

and

$$[R_2 m^2 - 2R_1 m] + \nu [R_1 - R_2 m] = \sigma . \quad (3.15)$$

Solving equations 3.14 and 3.15 for R_1 and R_2 ,

$$R_1 = \frac{\rho}{m(m-\nu)} \quad (3.16)$$

and

$$R_2 = \frac{\sigma}{m(m-\nu)} + \frac{R_1 (2m-\nu)}{m(m-\nu)} . \quad (3.17)$$

Expressing R_1 and R_2 in terms of basic parameters (i.e., a, b, c, ν, A, m),

$$R_1 = \frac{A}{c} \frac{(m^2 - am + b)}{m(m-v)} \quad (3.18)$$

and

$$R_2 = \frac{A}{cm^2(m-v)^2} [m^2(v-a) + m2b - vb] \quad (3.19)$$

$$\therefore \xi = L_1 + L_2 e^{-v\tau} + R_1 \tau^* e^{-m\tau^*} + R_2 e^{-m\tau^*}, \quad (3.20)$$

where R_1 and R_2 are given in equations 3.18, 3.19, and L_1 , L_2 can be evaluated from the initial conditions,

$$\xi = 0 \text{ at the time } \tau = 0; \quad (3.21)$$

$$\xi' = 1 \text{ at the time } \tau = 0. \quad (3.22)$$

From equation 3.20 and initial condition in equation 3.21,

$$L_1 + L_2 = -R_2 \quad (3.23)$$

Differentiating equation 3.20 with respect to τ^* ,

$$\xi' = L_2 e^{-v\tau^*} (v) + R_1 e^{-m\tau^*} + R_1 \tau^* e^{-m\tau^*} (-m) + R_2 e^{-m\tau^*} (-m). \quad (3.24)$$

From equation 3.24 and the initial condition in equation 3.22

$$\xi' \Big|_{\tau^*=0} = -vL_2 + R_1 + R_2(-m) = 1 \quad (3.25)$$

From the above equation,

$$L_2 = \frac{1}{v} [R_1 - R_2 m - 1] \quad (3.26)$$

From equations 3.23 and 3.26,

$$L_1 = -R_2 - \frac{1}{v} [R_1 - R_2 m - 1] \quad (3.27)$$

Expressing L_1 and L_2 in terms of basic parameters,

$$L_1 = \frac{-A}{cm^2(m-v)^2} [m^4 (\frac{1}{v} - \frac{c}{Av}) + 2m^3 (\frac{c}{A} - 1) + m^2 (v - \frac{b}{v} - \frac{c}{Av}) + m2b - vb] \quad (3.28)$$

and

$$L_2 = \frac{A}{cv(m-v)^2} [m^2 (1 - \frac{c}{A}) + 2vm (\frac{c}{A} - 1) + (av - b - \frac{c}{Av^2})] \quad (3.29)$$

$$\therefore \xi = L_1 + L_2 e^{-v\tau^*} + R_1 \tau^* e^{-m\tau^*} + R_2 e^{-m\tau^*}, \quad (3.20)$$

where L_1 , L_2 , R_1 and R_2 are as defined previously.

Instant of Maximum Deformation

Since the purpose of this analysis is to find the constraints on (a, b, c, d) such that the maximum normalized deformation ξ_{\max} is less than or equal to one, one needs to compute ξ_{\max} from equation 3.20. The instant τ_{\max}^* at which

ξ_{\max} is reached, if it exists, is to be found first.

Differentiation of equation 3.20 with respect to τ^* and equating the result to zero yields

$$vL_2 e^{-v\tau^*} = -mR_1 \tau^* e^{-m\tau^*} + (R_1 - mR_2) e^{-m\tau^*} . \quad (3.30)$$

$$\therefore e^{-v\tau^*} = e^{-m\tau^*} \left[\frac{-mR_1 \tau^*}{vL_2} + \frac{R_1 - mR_2}{vL_2} \right] . \quad (3.31)$$

Let

$$\frac{-mR_1}{vL_2} = L_3 \quad (3.32)$$

and

$$\frac{R_1 - mR_2}{vL_2} = L_4 . \quad (3.33)$$

Substituting these values in equation 3.31,

$$e^{-v\tau^*_{\max}} = e^{-m\tau^*_{\max}} [L_3 \tau^*_{\max} + L_4] , \quad (3.34)$$

which defines the instant τ^*_{\max} of maximum deformation ξ_{\max} .

When the numerical values of the parameters of concern are known, the application of graphical techniques is convenient.

From equation 3.34,

$$e^{(m-\nu)\tau_{\max}^*} = L_3 \tau_{\max}^* + L_4 \quad (3.35)$$

Let

$$z = [m-\nu]\tau_{\max}^* \quad (3.36)$$

From equations 3.35 and 3.36,

$$e^z = \frac{L_3 z}{(m-\nu)} + L_4 \quad (3.37)$$

Substituting the values of L_3 and L_4 from equations 3.32 and 3.33,

$$e^z = \frac{-mR_1 z}{\nu L_2 (m-\nu)} + \frac{R_1 - mR_2}{\nu L_2} \quad (3.38)$$

The above equation is of the form

$$e^z = \theta z + \psi \quad (3.39)$$

Plotting e^z once and for all renders the solution as the intersect between a straight line and the curve e^z .

From the numerical values of the constants θ and ψ , which represent the slope and intercept on the y axis, respectively, of the straight line represented by the right

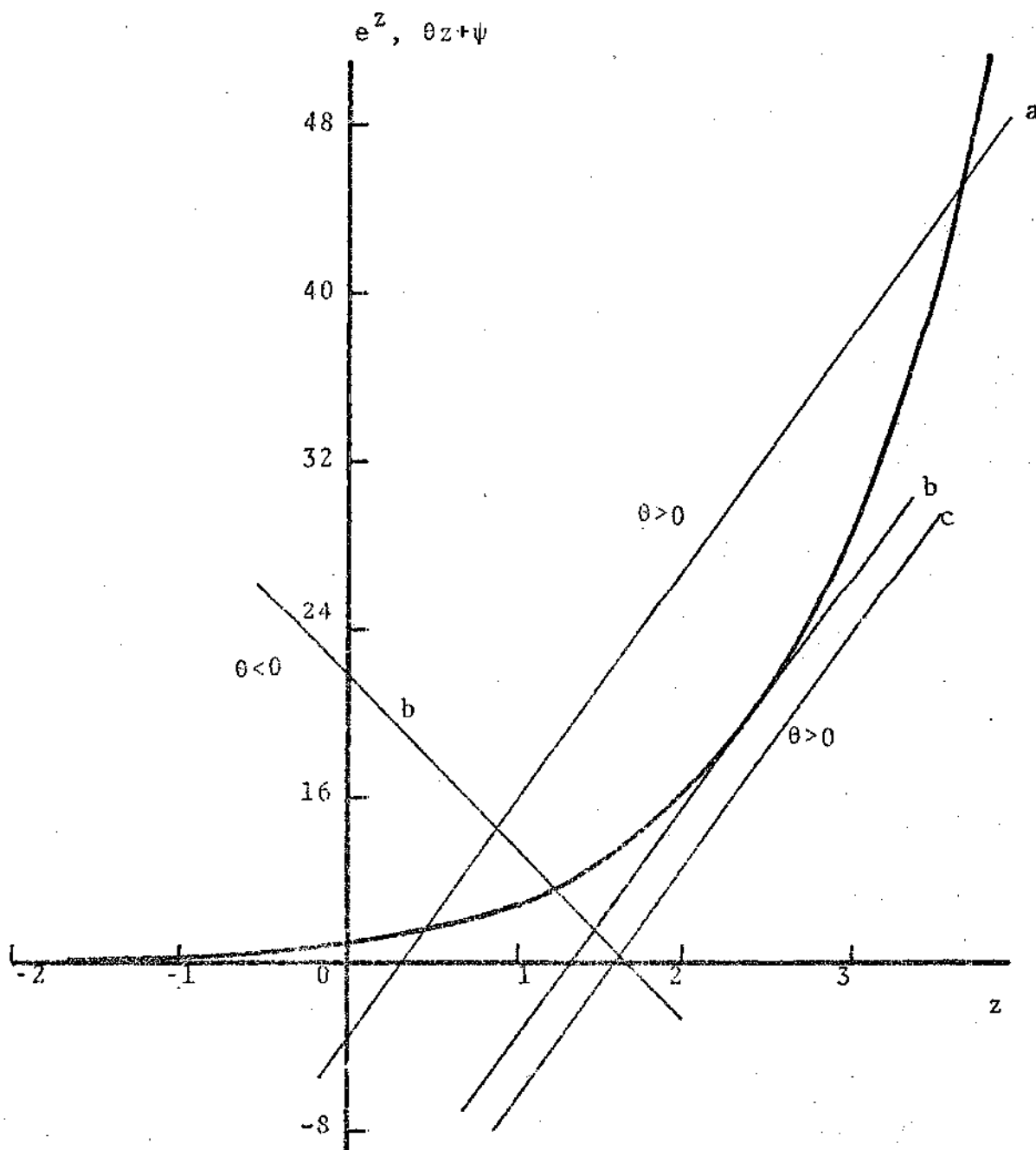


Figure 4. Graphical Solution to Equation 3.39
 a: Two Possible Solutions for Real $z > 0$
 b: One Possible Solution for Real $z > 0$
 c: No Real Solution

hand side of equation 3.39, some broad conclusions about the τ_{\max}^* when the deformation is maximum can be drawn. If the slope is negative, the straight line will definitely intercept the e^z curve at only one point, and there is one and only one solution for the time τ^* when the deformation is maximum. On the other hand, if the slope is positive, depending on the values of θ and ψ , the straight line may intercept, may be tangential or may not touch the curve e^z , thus giving either two values of z (and hence τ_{\max}^*) when the deformation is maximum, or one value or no real value, respectively.

A second method for the solution of equation 3.34 is given below. An analytical expression for τ_{\max}^* can be found (as shown below), but this expression will have only a limited applicability, i.e., it can be applied only when $L_3 \tau_{\max}^*$ has a small value.

Taking natural logarithm on both sides of equation 3.34 and rearranging,

$$\tau_{\max}^* (m-\nu) = \log_e [L_3 \tau_{\max}^* + L_4]. \quad (3.40)$$

Noting that

$$\log_e (a+x) = \log_e a + 2 \left[\frac{x}{2a+x} + \frac{1}{3} \left(\frac{x}{2a+x} \right)^3 + \frac{1}{5} \left(\frac{x}{2a+x} \right)^5 + \dots \right]$$

and making first order approximation, equation 3.40 becomes

$$\tau_{\max}^* [m-v] = \log_e L_4 + \frac{2L_3 \tau_{\max}^*}{2L_4 + L_3 \tau_{\max}^*} . \quad (3.41)$$

Letting

$$L_3 \tau_{\max}^* = x, \quad (3.42)$$

$$\left[\frac{m-v}{L_3} \right] = L_5 \quad (3.43)$$

and

$$\log_e L_4 = L_6 , \quad (3.44)$$

and substituting these values in equation 3.41, we get

$$xL_5 = L_6 + \frac{2x}{2L_4 + x} . \quad (3.45)$$

Rearranging the terms,

$$x^2 L_5 + x[2L_4 L_5 - L_6 - 2] - 2L_4 L_6 = 0 . \quad (3.46)$$

Solving the above quadratic equation for x,

$$x = \left(\frac{1}{L_5} + \frac{L_6}{2L_5} - L_4 \right) \pm \sqrt{\left(\frac{1}{L_5} + \frac{L_6}{2L_5} - L_4 \right)^2 + \frac{2L_4 L_6}{L_5}} . \quad (3.47)$$

From equations 3.42 and 3.47,

$$\tau_{\max}^* = \left[\frac{1}{L_5 L_3} + \frac{L_6}{2L_5 L_3} - \frac{L_4}{L_3} \right] \pm \sqrt{\left(\frac{1}{L_5 L_3} + \frac{L_6}{2L_5 L_3} - \frac{L_4}{L_3} \right)^2 + \frac{2L_4 L_6}{L_5 L_3^2}}. \quad (3.48)$$

Substituting the values of L_3 , L_4 , L_5 and L_6 from equations 3.32, 3.33, 3.43 and 3.44 in equation 3.48 and simplifying, we obtain

$$\tau_{\max}^* = \frac{2 + \log_e \frac{R_1 - mR_2}{vL_2}}{2(m-v)} + \left(\frac{R_1 - mR_2}{mR_1} \right) \pm \sqrt{\left(\frac{2 + \log_e \frac{R_1 - mR_2}{vL_2}}{2(m-v)} + \frac{R_1 - mR_2}{mR_1} \right)^2 - \frac{2(R_1 - mR_2)}{(m-v)mR_1} \log_e \left(\frac{R_1 - mR_2}{vL_2} \right)}. \quad (3.49)$$

Equation 3.49 can be written as

$$\tau_{\max}^* = \lambda \pm \sqrt{\lambda^2 + \mu}, \quad (3.50)$$

where

$$\lambda = \frac{2 + \log_e \frac{R_1 - mR_2}{vL_2}}{2(m-v)} + \left(\frac{R_1 - mR_2}{mR_1} \right) \quad (3.51)$$

and

$$\mu = -\frac{2(R_1 - mR_2)}{(m-v)mR_1} \log_e \left(\frac{R_1 - mR_2}{vL_2} \right). \quad (3.52)$$

In the actual impact situations, only real, non-negative values of time will be considered. If both the values of time are non-negative and real, then the smaller of them will be chosen because this represents the case when the deformation has reached the maximum value for the first time.

Substituting the value of time τ_{\max}^* obtained from the equation 3.49 in the equation 3.20 gives the maximum deformation.

Parameter Constraints

From equation 3.20,

$$\xi = L_1 + L_2 e^{-\nu\tau^*} + e^{-m\tau^*} (R_1 \tau_{\max}^* + R_2) .$$

τ_{\max}^* at the instant of maximum deformation, from equation 3.34 is

$$e^{-\nu\tau_{\max}^*} = e^{-m\tau_{\max}^*} [L_3 \tau_{\max}^* + L_4] .$$

From the above equation,

$$e^{-m\tau_{\max}^*} = \frac{e^{-\nu\tau_{\max}^*}}{[L_3 \tau_{\max}^* + L_4]} . \quad (3.53)$$

Substituting this value of $e^{-m\tau^*}$ in equation 3.20,

$$\xi_{\max} = L_1 + e^{-\nu\tau_{\max}^*} \left\{ L_2 + \frac{R_1 \tau_{\max}^* + R_2}{L_3 \tau_{\max}^* + L_4} \right\} . \quad (3.54)$$

Consider the term $e^{-\nu\tau_{\max}^*}$, where

$$\nu = \frac{\text{elastically reversible force}}{\text{irrecoverable force (i.e., dissipative force)}}$$

or

$$\nu = \frac{K_1 \delta}{\tau_{\max}^* C V_0}$$

For a Hookian elastic material $\nu = \infty$ and for a Newtonian viscous fluid $\nu = 0$. For an actual material ν lies in between. Generally for a visco-elastic material the recoverable force is quite large compared to the dissipative force. Hence a value of 10 taken for ν , which gives an order of magnitude difference between the above two forces is actually a conservative estimate. For all the cases observed on the analog computer, τ_{\max}^* was greater than two. Hence, a value of $\tau_{\max}^* = 2$, which is a conservative lower bound for the time at which maximum deformation occurs, may be taken to find the relative significance of the second term in equation 3.54. Substituting the above values for ν and τ_{\max}^* in equation 3.54 gives, with $\tau_{\max}^* \nu = 20$.

$$\xi_{\max} = L_1 + \frac{1}{e^{20}} \left[L_2 + \frac{R_1 \tau_{\max}^* + R_2}{L_3 \tau_{\max}^* + L_4} \right]$$

For an order of magnitude comparison the term $\frac{1}{e^{20}} \left[L_2 + \frac{R_1 \tau_{\max}^* + R_2}{L_3 \tau_{\max}^* + L_4} \right]$ was calculated for known values of parameters ($a = 26.6$,

$b = 66.66$, $c = 8$, $d = 80$, $m = 3.1$ and $A = 9.9$ taken from the analog computer solution) and found to be equal to $.876 \times 10^{-9}$. Hence, the second term can be neglected without the loss of accuracy, and $\xi_{\max} = 1 \geq L_1$ is the constraint that relates system parameters to pulse shape parameters such that the padding thickness remains non-negative.

$$\xi_{\max} = \frac{-A}{cm^2(m-v)^2} [m^4 \left(\frac{1}{v} - \frac{C}{Av}\right) + 2m^3 \left(\frac{C}{A} - 1\right) + m^2 \left(v - \frac{b}{v} - \frac{C}{A}v\right) + m2b - vb] . \quad (3.55)$$

The above equation can be used to find the parametric constraints, i.e., given the values of the other parameters, the limiting value of one of the parameters which makes $\xi_{\max} = 1$ can be found from this. For example, given $a = 26.6$, $c = 8$, $d = 80$, $m = 3.1$ and $A = 9.9$, the limiting value of b computed from the above equation is 80.

Energy Absorption

Energy absorption during impact is given by

$$W = m_1 v_0^2 \int_0^{\tau^*} \phi \xi' d\tau^* \quad (3.56)$$

$$\omega = \frac{W}{m_1 v_0^2} = \int_0^{\tau^*} \phi \xi' d\tau^* . \quad (3.57)$$

Substituting the values of ϕ and ξ' from equation 3.30,

$$W = -AvL_2 \int_0^{\tau^*} \tau^* e^{-(v+m)\tau^*} d\tau^* - AmR_1 \int_0^{\tau^*} \tau^{*2} e^{-2m\tau^*} d\tau^* + A(R_1 - mR_2) \int_0^{\tau^*} \tau^* e^{-2m\tau^*} d\tau^* \quad (3.58)$$

Integrating,

$$\begin{aligned} \omega = & -AvL_2 \left[\frac{-e^{-(v+m)\tau^*} \{1 + \tau^*(v+m)\}}{(v+m)^2} + \frac{1}{(v+m)^2} \right] \\ & - AmR_1 \left[\frac{-e^{-2m\tau^*}}{4m^3} \{2m^2 \tau^{*2} + 1 + 2m\tau^*\} + \frac{1}{4m^3} \right] \\ & + A(R_1 - mR_2) \left[\frac{-e^{-2m\tau^*} \{1 + \tau^*(2m)\}}{(2m)^2} + \frac{1}{(2m)^2} \right] \quad (3.59) \end{aligned}$$

Rearrangement and simplification gives the final expression

$$\begin{aligned} \omega = & e^{-(v+m)\tau^*} \left[\frac{AvL_2 \{1 + \tau^*(v+m)\}}{(v+m)^2} + \frac{e^{-2m\tau^*}}{4m^2} \right] \\ & \{2Am^2 \tau^{*2} (R_1 + R_2) + AmR_2\} - \frac{AR_2}{4m} \frac{AvC_2}{(v+m)^2} \quad (3.60) \end{aligned}$$

The above analytical expression suggests an alternate means of calculating the energy absorption, in addition to the one using an analogue computer.

CHAPTER IV

RESULTS

An impact situation is considered in which an object of mass 10 kg, such as human head and neck with protective system hits an automobile part (front panel) with a velocity of 10 m/sec. The panel is protected by a 2 cm-thick padding of Valox 310 (unreinforced) thermoplastic polyester. The visco-elastic parameters for the panel are chosen to be:

$$m = 100 \text{ kg,}$$

$$K_3 = 50 \times 10^6 \text{ N/m, and}$$

$$C_3 = 10 \times 10^6 \text{ Ns/m.}$$

The system parameters for Valox 310 (unreinforced) thermoplastic polyester are [19] [9]

$$K_1 = 20 \times 10^6 \text{ N/m,}$$

$$K_2 = 20 \times 10^6 \text{ N/m,}$$

$$C_1 = 4000 \text{ Ns/m, and}$$

$$C_2 = 6000 \text{ Ns/m.}$$

The reference time is $\delta/V_0 = 2 \times 10^{-3}$ seconds and the impact energy is $m_1 V_0^2 / 2 = 500 \text{ Nm}$.

The above impact parameters yield the following values for the nondimensional groups defined by equations 2.27 through 2.36:

impactor characteristics:

$$A = 0; B = 1;$$

padding characteristics:

$$a = 26.6; b = 66.66; c = 8; d = 80; e = 8; \text{ and}$$

support characteristics:

$$\alpha = 0.2; \beta = 2; \gamma = 0.1.$$

To find the effect of padding parameters on (1) padding deformation history during impact, (2) impact force variation with time, (3) dynamic stress-strain characteristic of padding systems, (4) energy absorption during impact, one of the four parameters is varied, while keeping the other three fixed at the above indicated values. Each of the above four responses is described below with reference to the corresponding figures.

Graphical Presentation

Padding Deformation History During Impact

The set of Figures 5 through 8 depicts the normalized padding deformation ξ as a function of normalized time τ^* with a , b , c , and d (in that order) as parameters.

Impact Force Variation with Time

The set of Figures 9 through 12 depicts the normalized force ϕ acting at the interface between the padding and its support, as a function of normalized time τ^* with a , b , c , and d (in that order) as parameters.

Dynamic Stress-Strain Characteristics of Four Parameter
Padding Systems

The set of Figures 13 through 16 represents the normalized force ϕ as a function of normalized deformation ξ with a, b, c, and d (in that order) as parameters.

Energy Absorption During Impact

The set of Figures 17 through 20 represents the normalized energy absorptions ω as a function of normalized time τ^* , with a, b, c, and d (in that order) as parameters. The normalized energy absorption is

$$\omega = \tau^* \int_0^{\tau^*} \phi \xi' d\tau^* \quad (4.1)$$

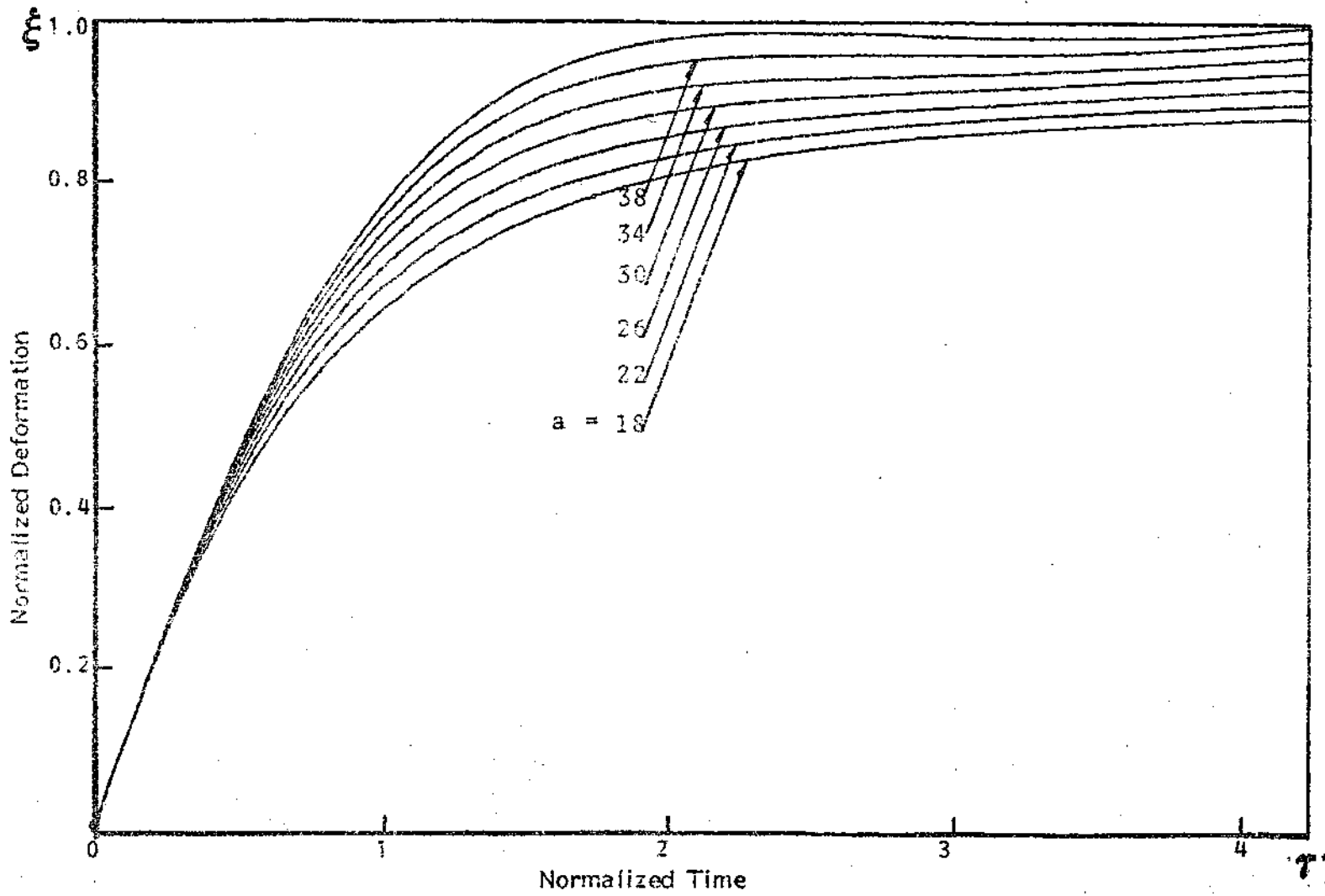


Figure 5. Padding Deformation History During Impact, Effect of Parameter a .

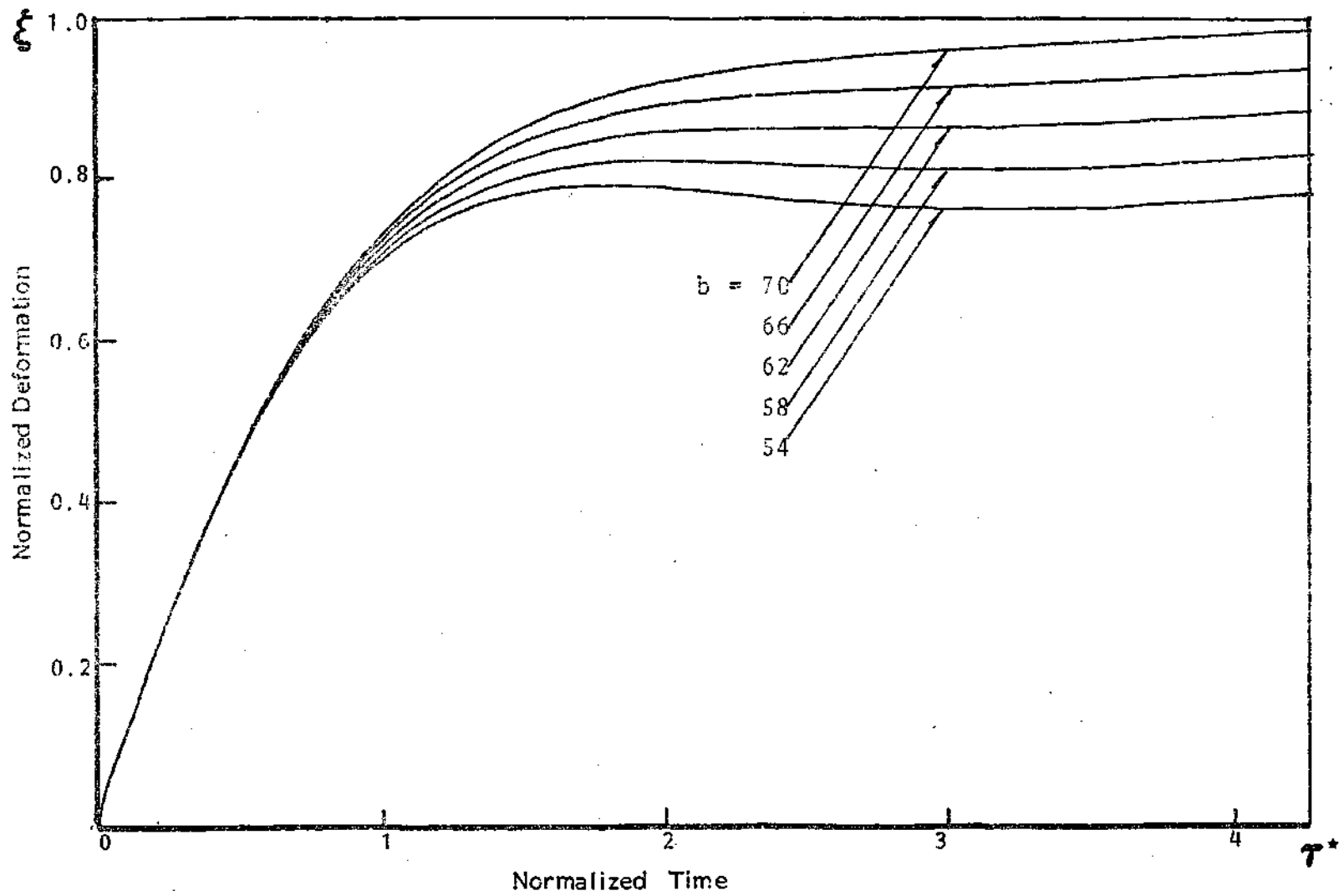


Figure 6. Padding Deformation History During Impact, Effect of Parameter b .

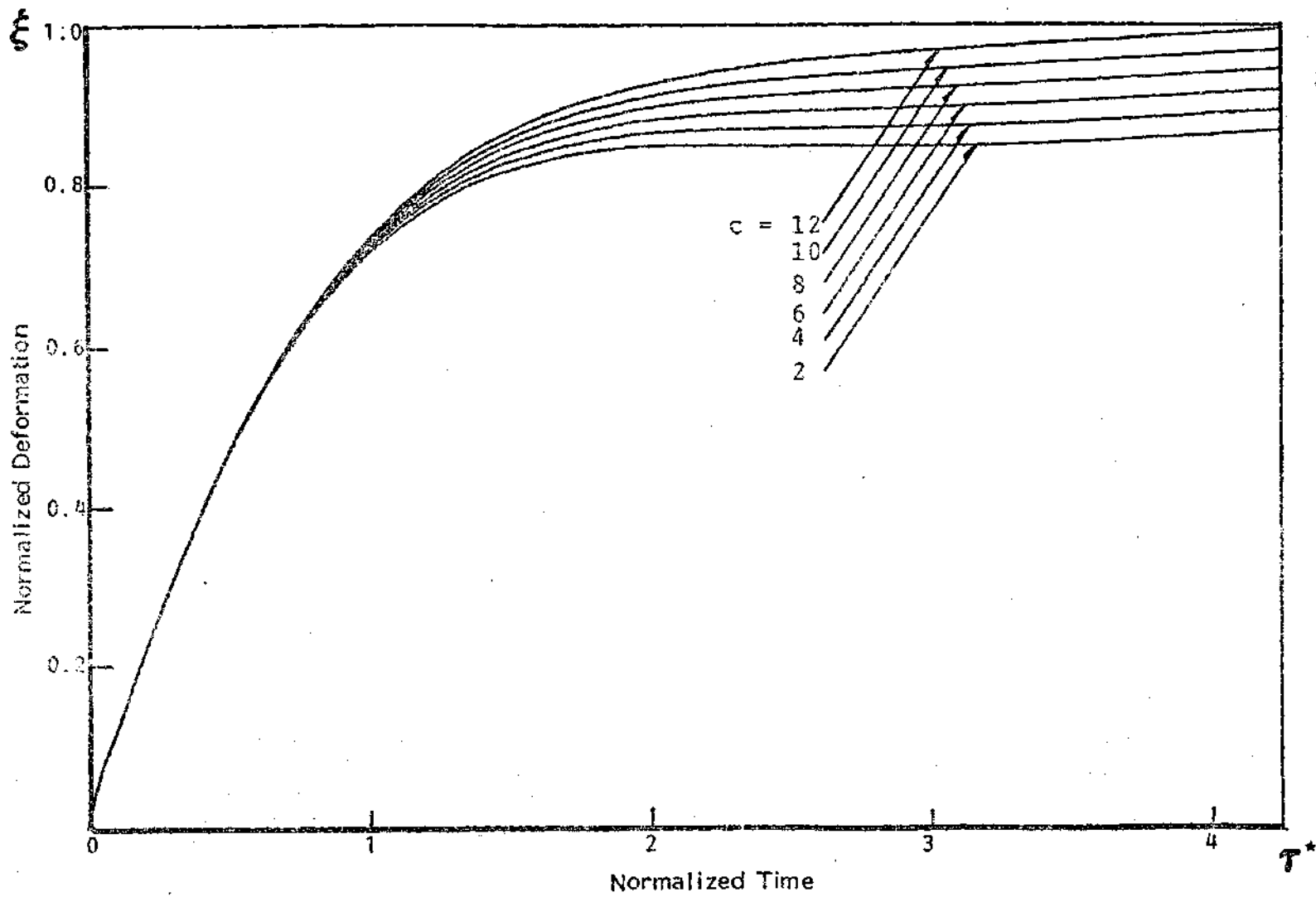


Figure 7. Padding Deformation History During Impact, Effect of Parameter c .

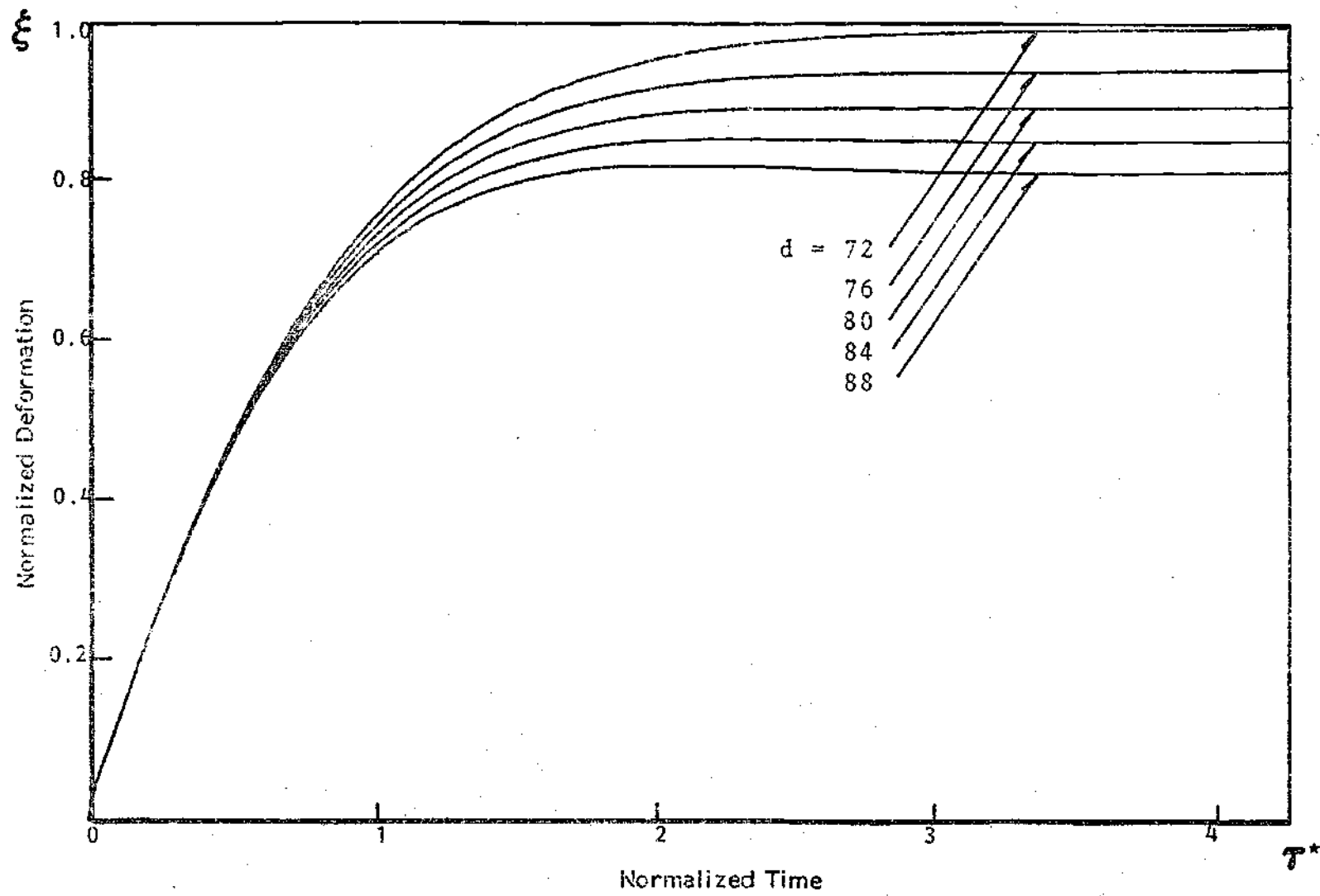


Figure 8. Padding Deformation History During Impact, Effect of Parameter d.

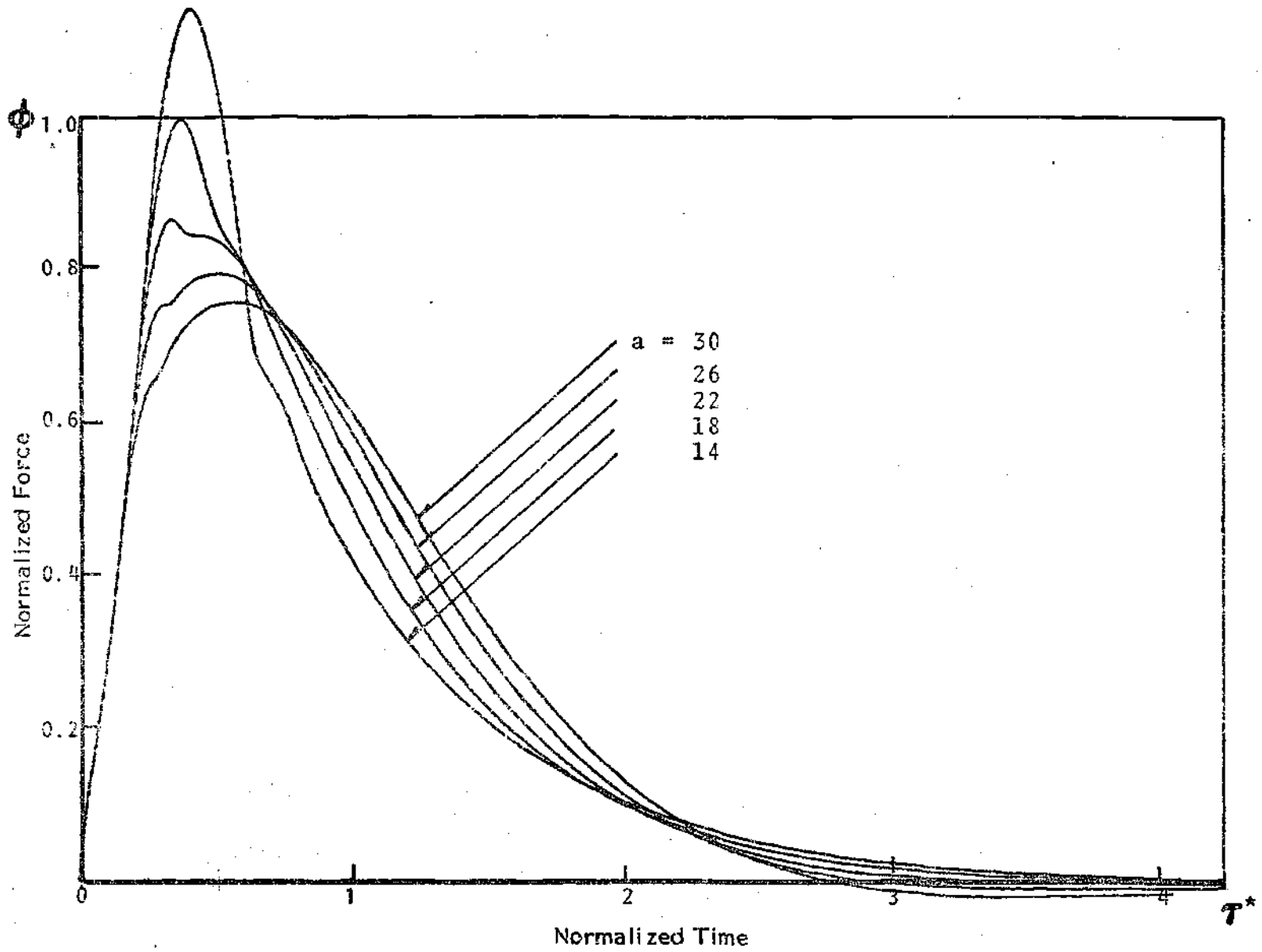


Figure 9. Impact Force As A Function of Time with a as Parameter.

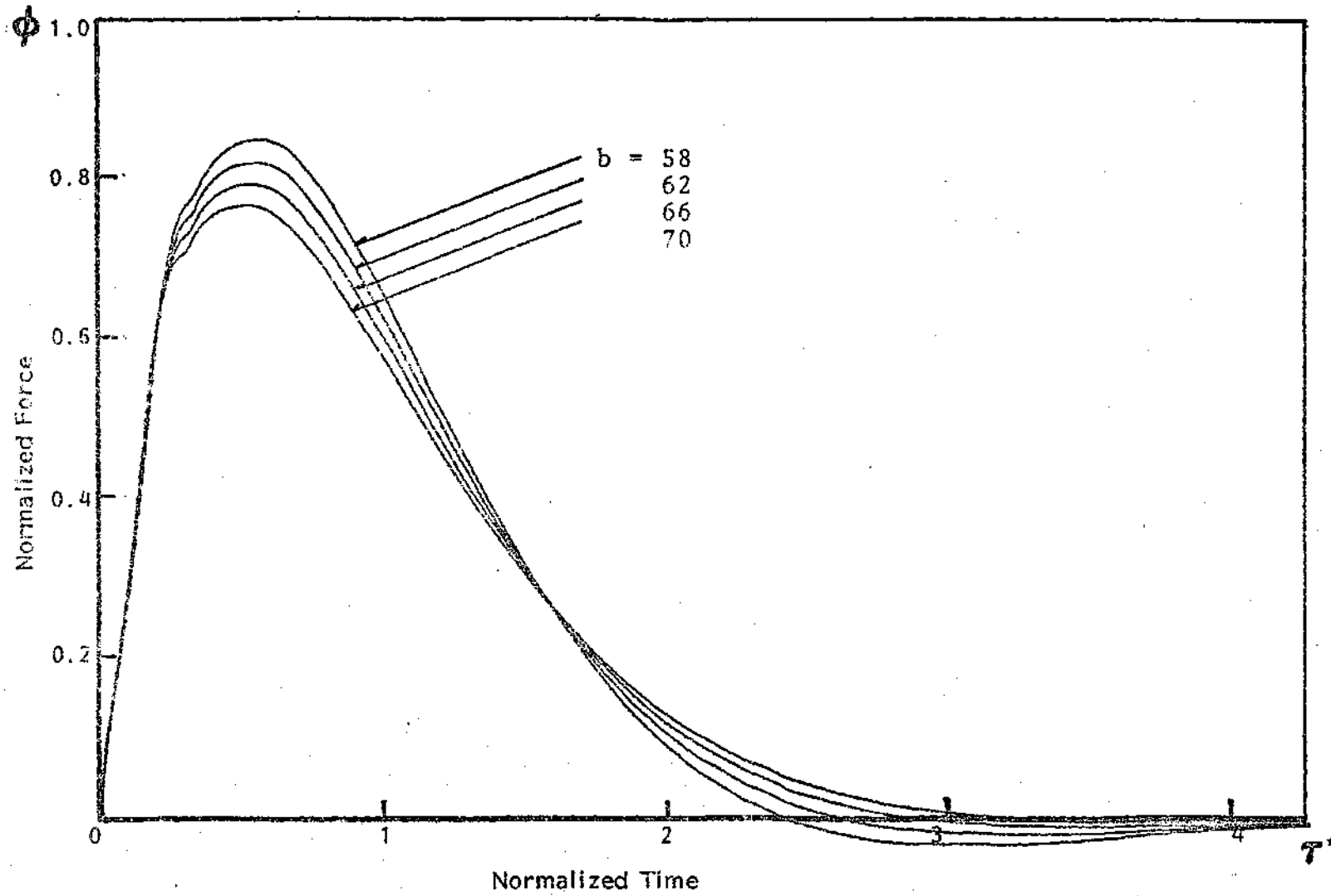


Figure 10. Impact Force As A Function of Time with b as Parameter.

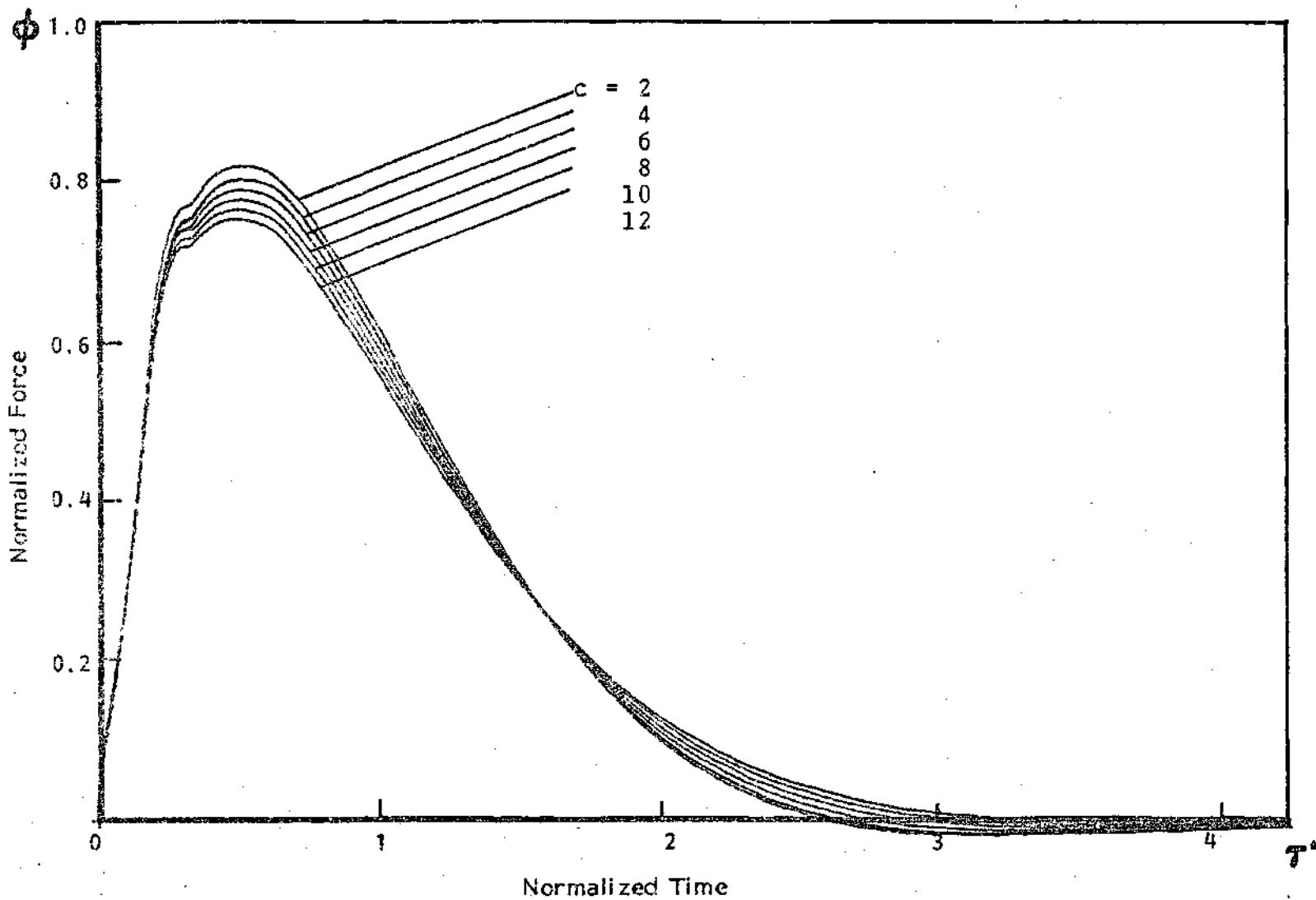


Figure 11. Impact Force As A Function of Time with c as Parameter.

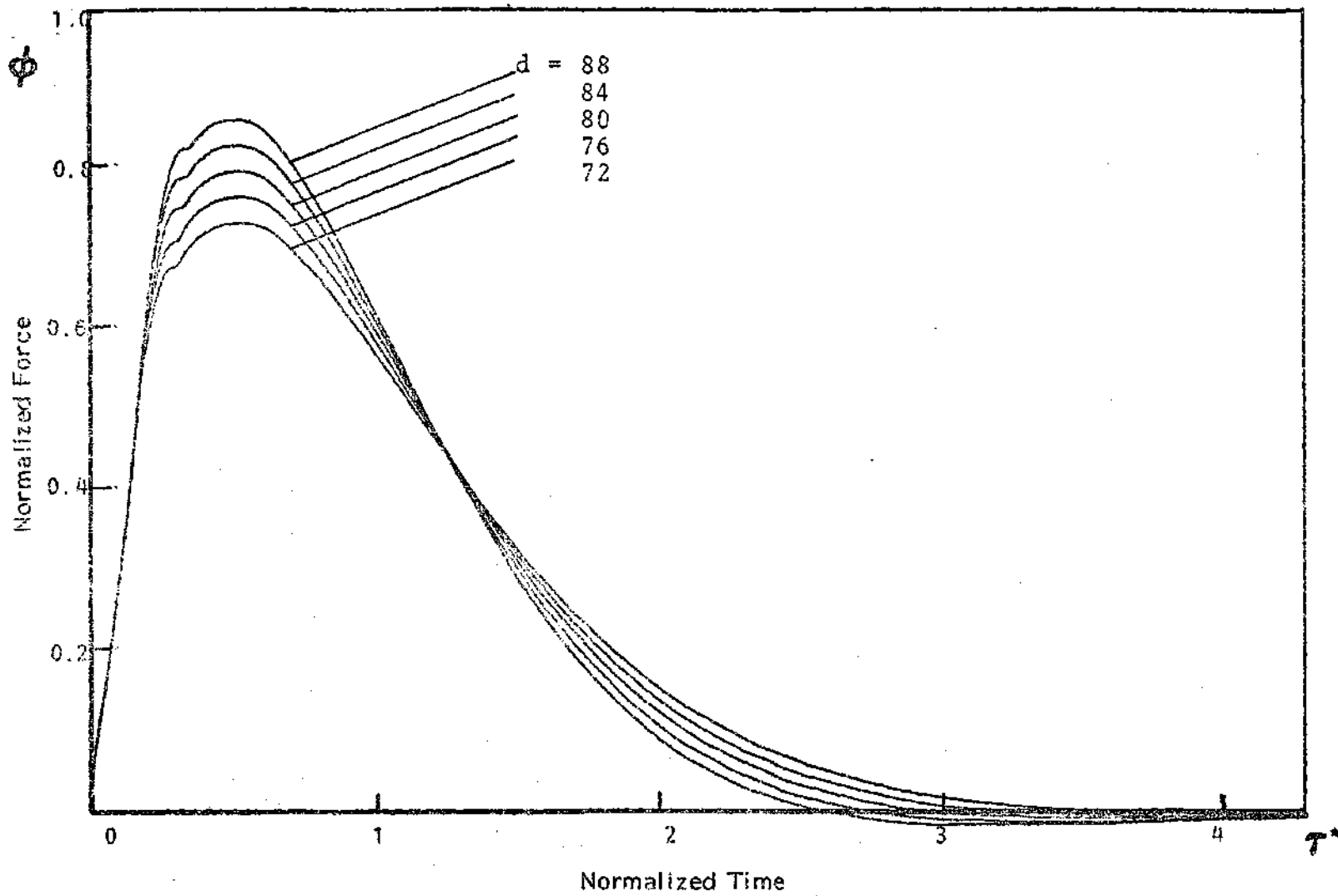


Figure 12. Impact Force As A Function of Time with d as Parameter.

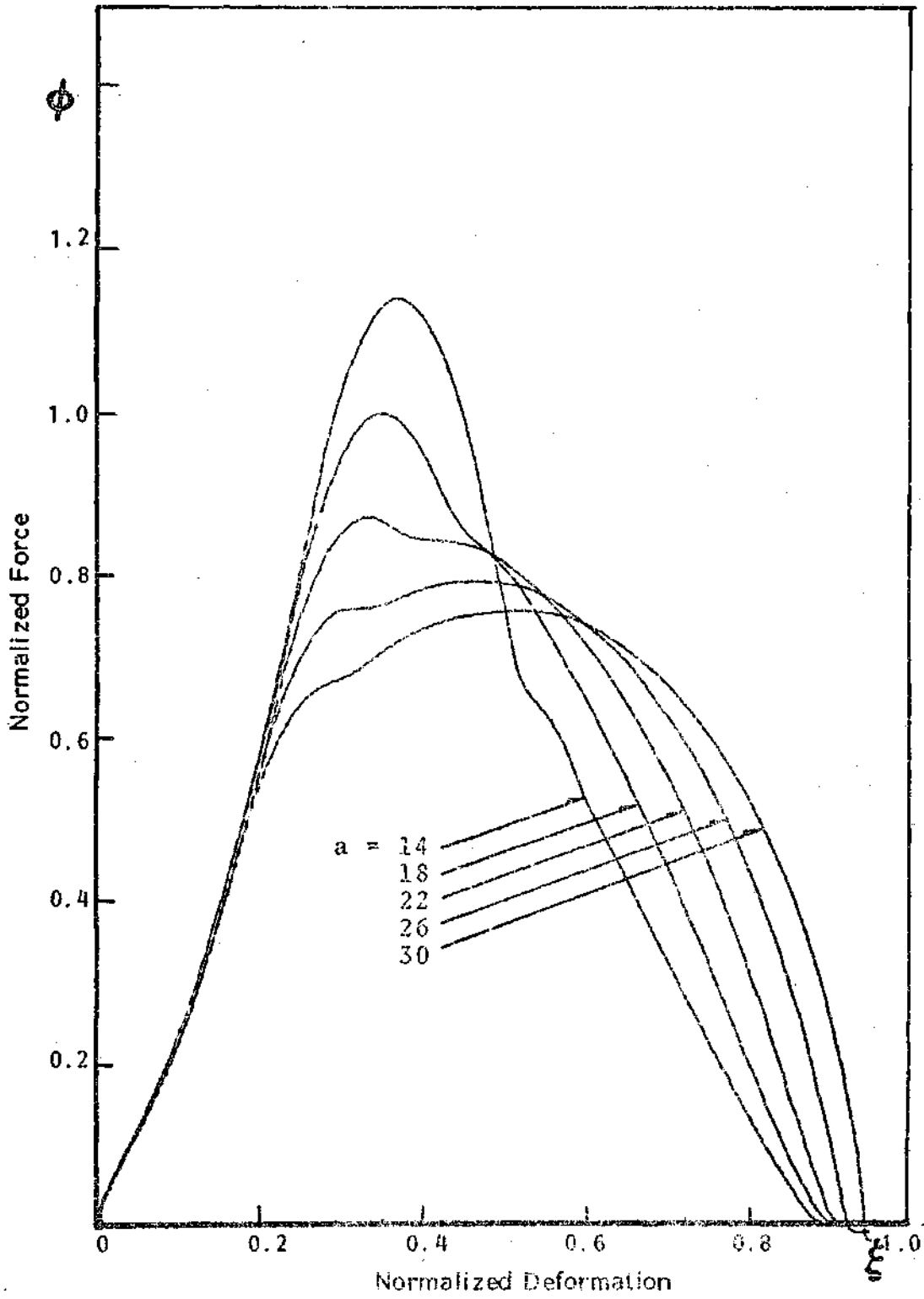


Figure 13. Stress-Strain Response As A Function of Parameter a .

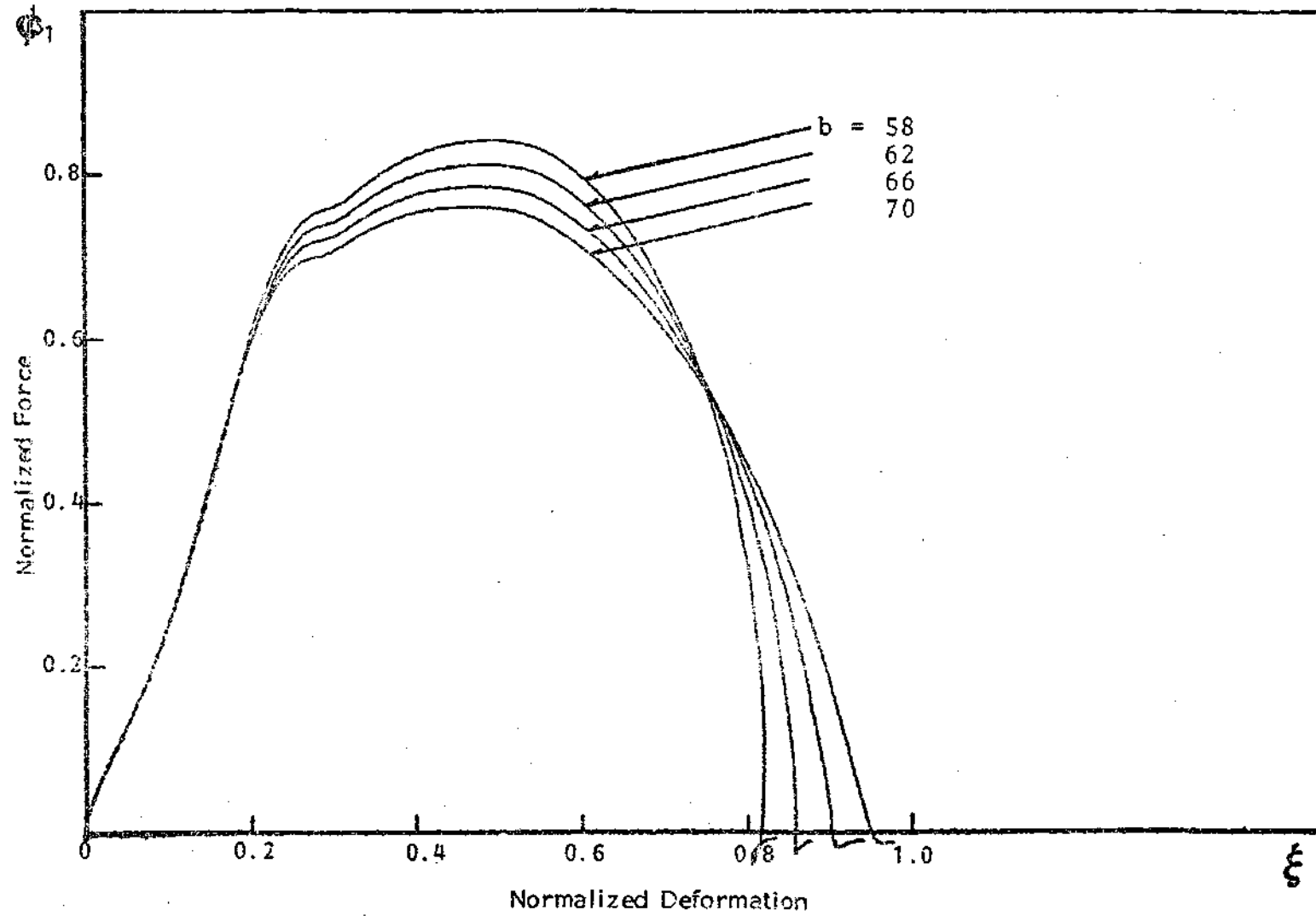


Figure 14. Stress-Strain Response As A Function of Parameter b .

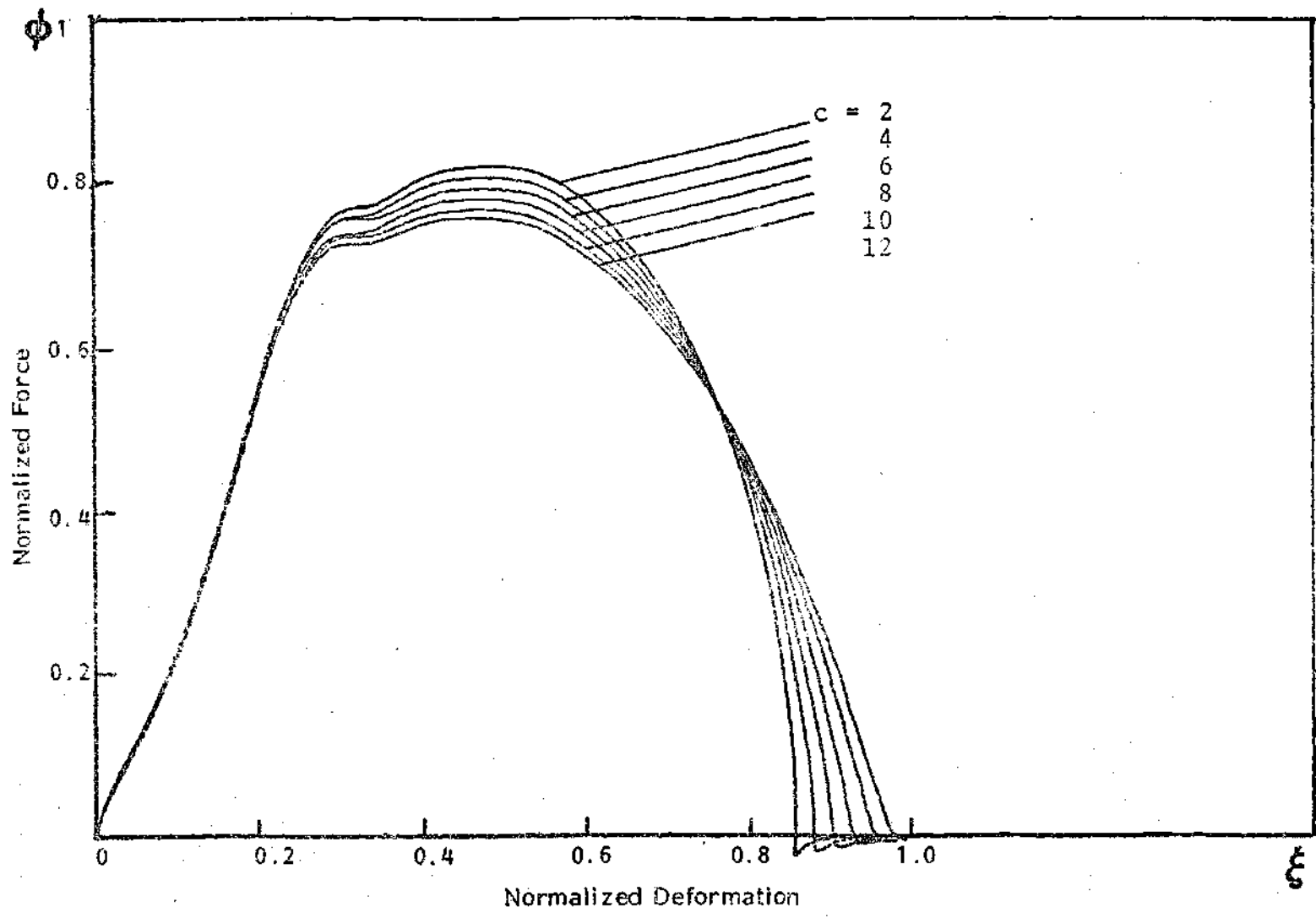


Figure 15. Stress-Strain Response As A Function of Parameter c.

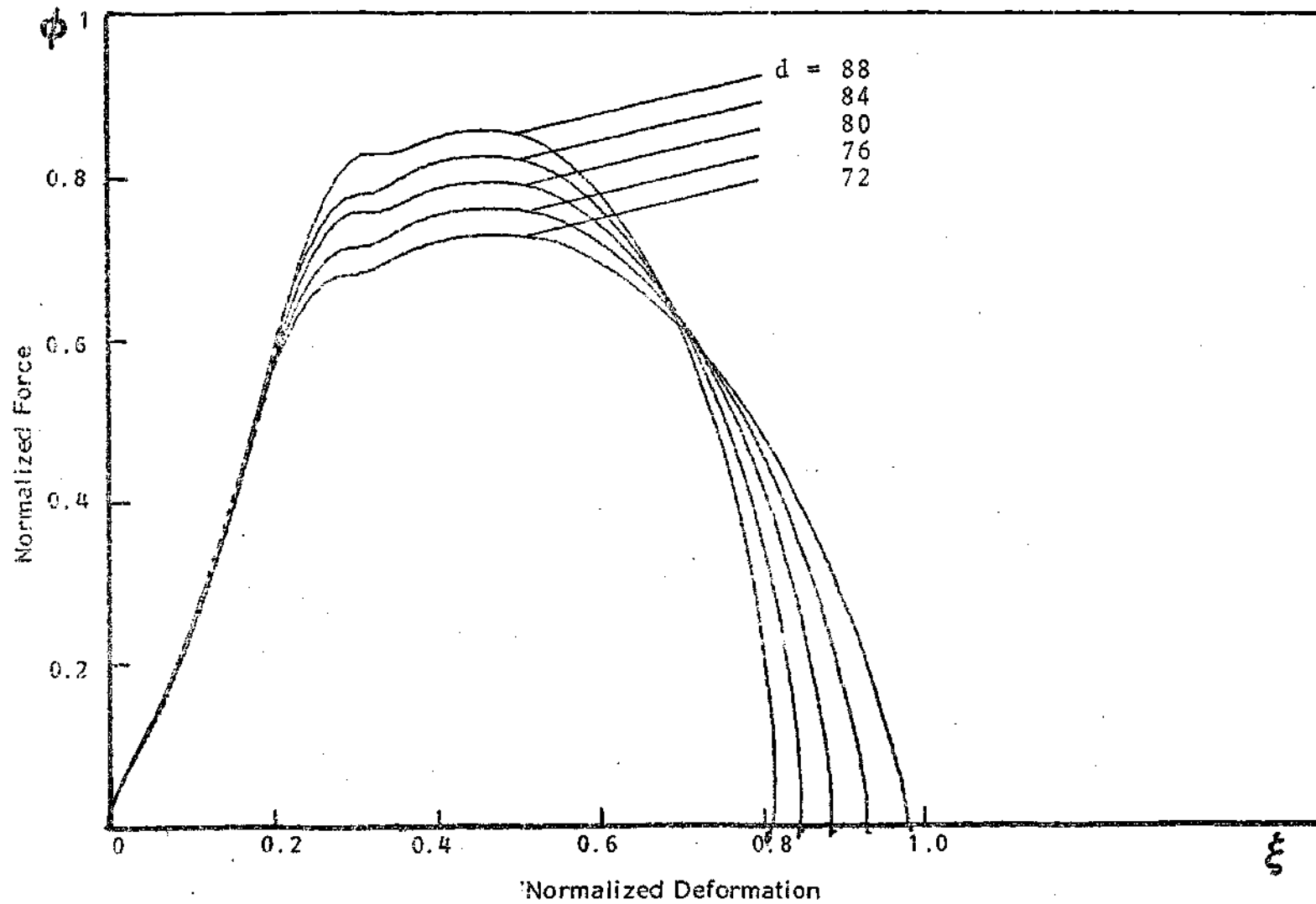


Figure 16. Stress-Strain Response As A Function of Parameter d .

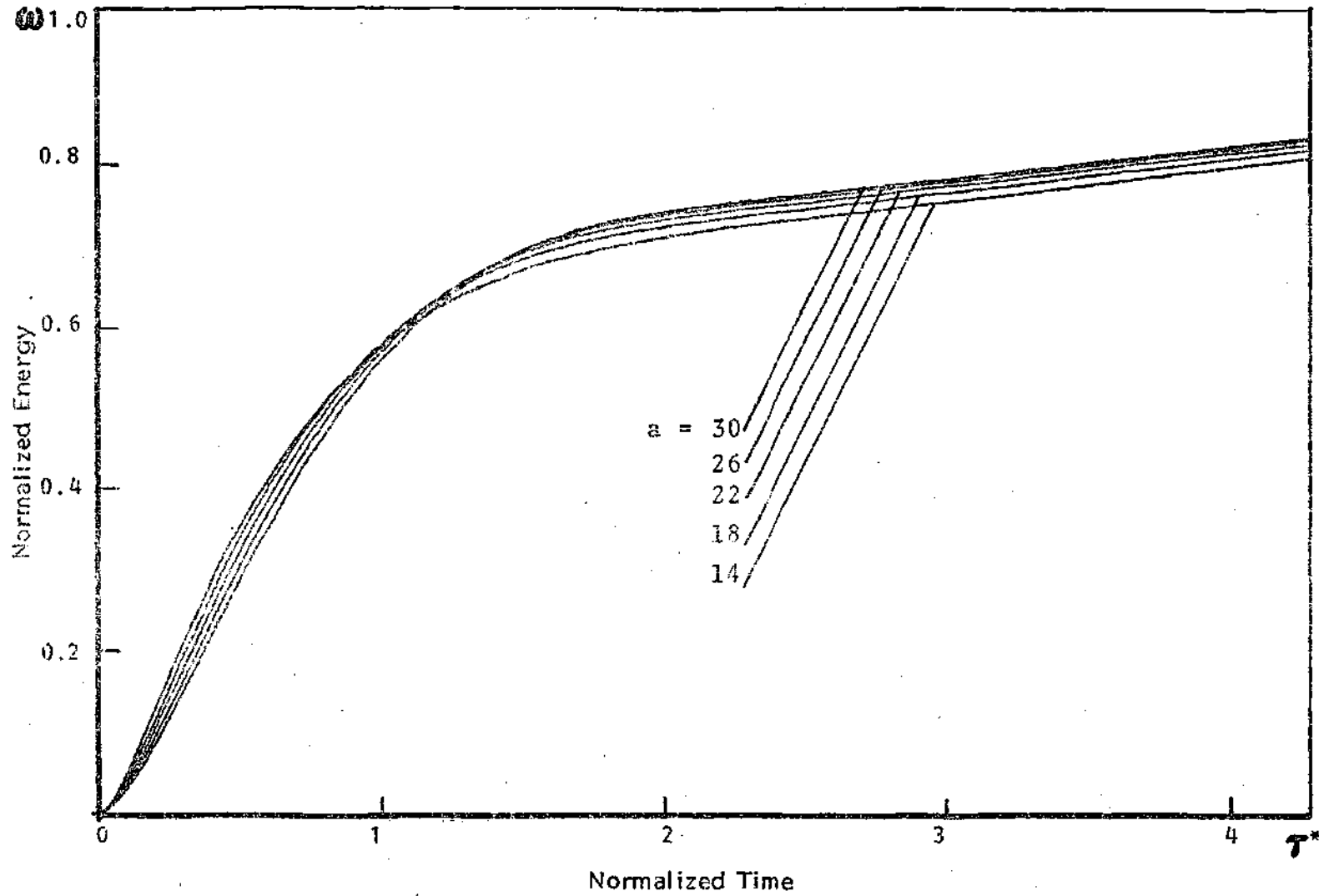


Figure 17. Energy Absorption with a As Parameter.

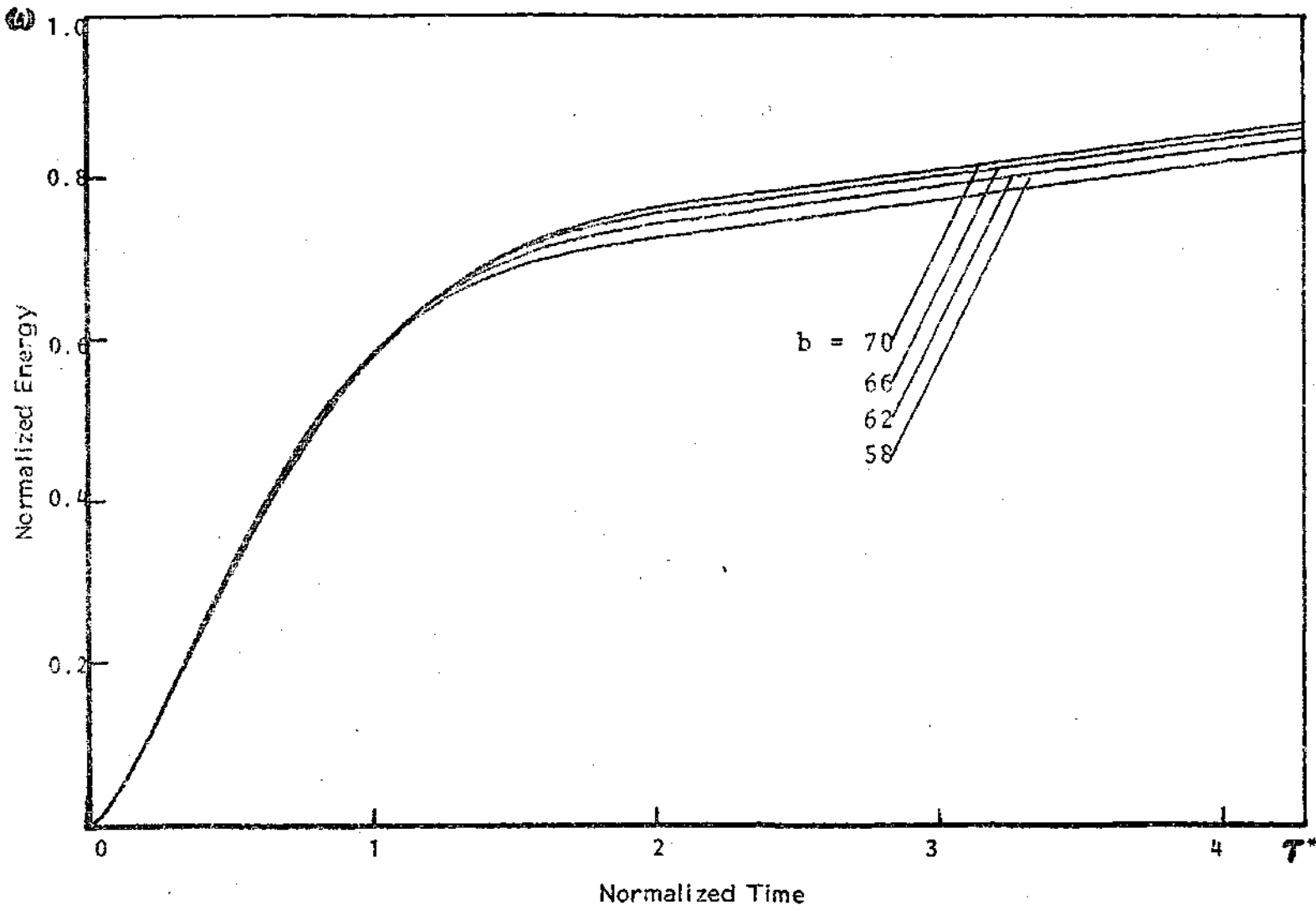


Figure 18 Energy Absorption with b as Parameter.

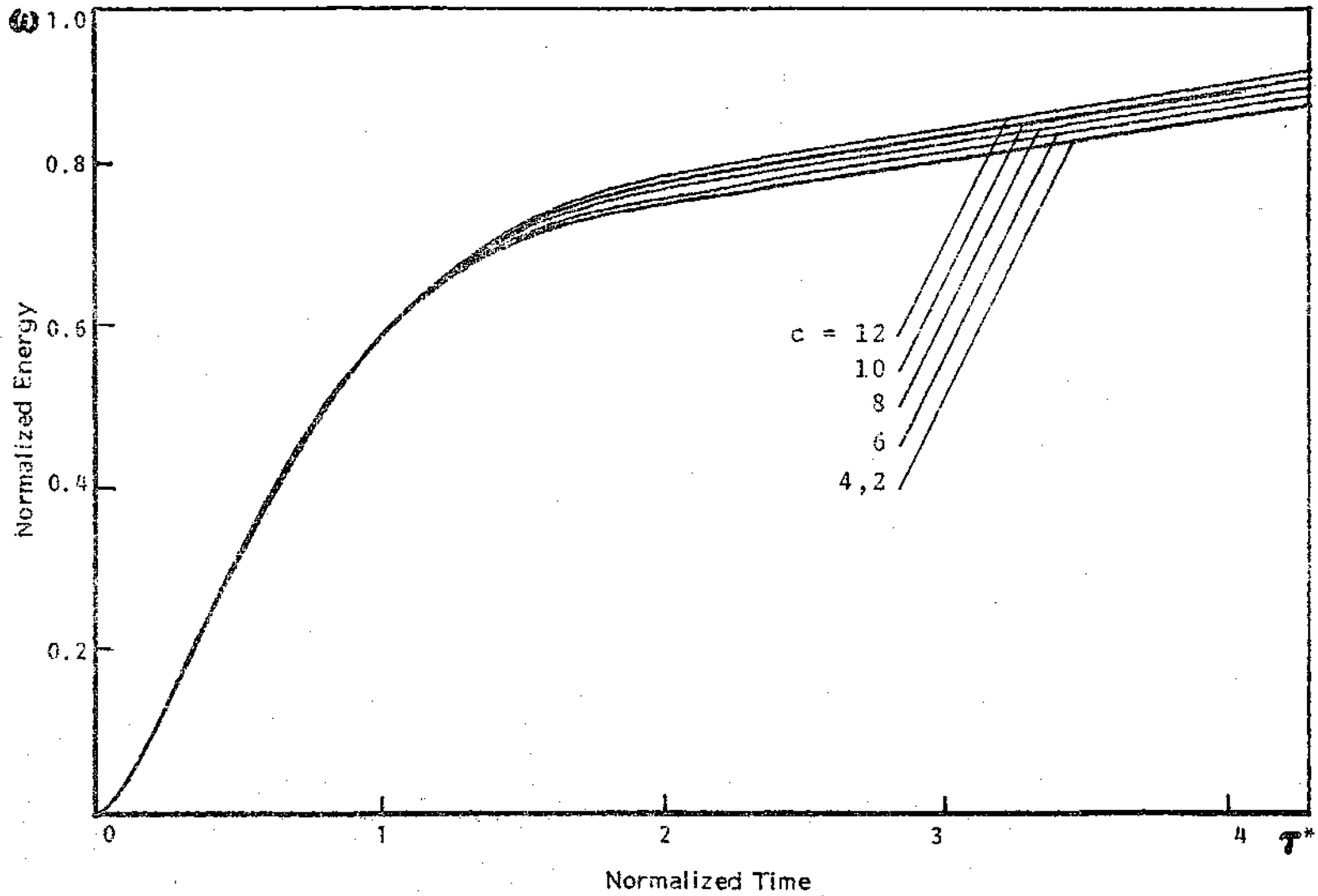


Figure 19. Energy Absorption with c As Parameter.

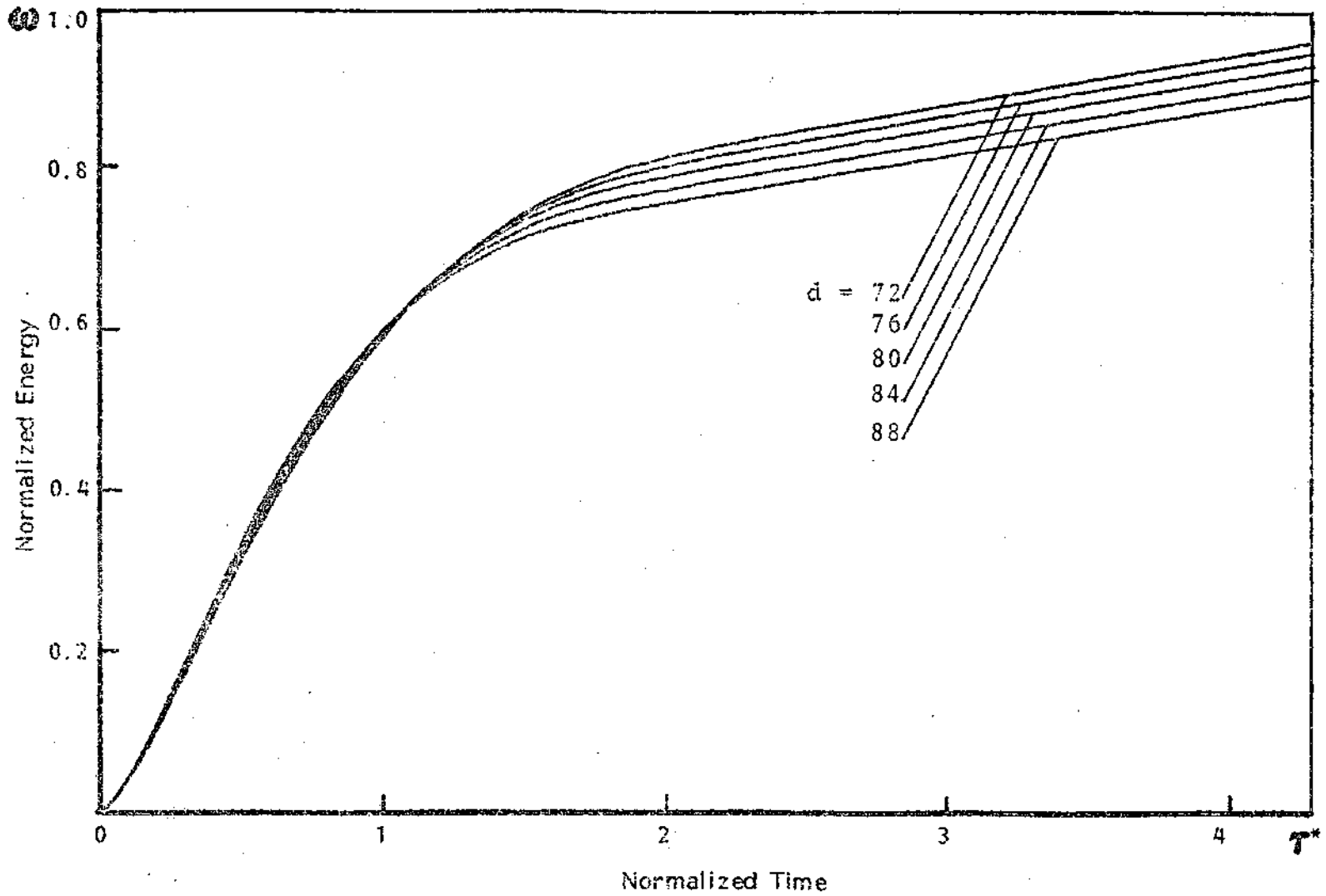


Figure 20. Energy Absorption with d As Parameter.

CHAPTER V

DISCUSSION

The significance of the information obtained from the modeling analysis, from the analogue computer solutions and its results is discussed below.

As mentioned in the introduction, the main function of the protective padding materials is the mitigation of impact injury. Padding materials are used to achieve the above objective by absorbing impact energy as dissipative energy or by storing impact energy partially during the first phase of impact, and releasing the stored energy during the latter phase of impact. By the virtue of the above qualities the padding materials are able to reduce (1) the amount of energy entering the body, and (2) the peak forces encountered.

Fibrous materials absorb energy effectively through friction between crossing fibers and through stressing individual fibers beyond their elastic yield limit either in tension or in bending or both. The ability of the padding to absorb energy is quantitatively assessed through the bulk description in terms of its viscous damping coefficients in equation 2.12.

The energy stored and dissipated in the fabric at any time is

$$\begin{aligned}
 W &= \int_0^{(x_1-x_2)(\tau)} F_2 d(x_1-x_2) \\
 &= mv_0^2 \int_0^{\tau^*} \phi \xi' d(\tilde{\tau}^*) \quad (5.1)
 \end{aligned}$$

The integral of equation 5.1 can be evaluated directly from the analogue computer and is proportional to the area under dynamic stress-strain curves.

In any impact situation the first few milliseconds are the most important period. The peak force, which is an important injury criterion, occurs during this period. Therefore, the ability of the material to absorb impact energy during this crucial initial period is an important criterion in grading the padding materials for impact protection. From the study of Figures 17 through 20, it can be observed that the variation of the parameters a, b, c, and d changes the amount of energy absorption during the first 10 milliseconds by about 3 to 7 percent. This variation in the energy absorption is quite significant. From the above figures, it can also be noted that the variation of the parameter d has the greatest effect on the variation of the energy absorption followed by c, b, and a, in that order. The study of Figures 9 through 12 and Figures 17 through 20 shows that the increase of parameters a, b, c, and the decrease of the parameter d, increase the amount of energy absorption and reduce the peak force occurring during the crucial initial

period. Therefore, if one has to choose between two padding materials, the selection of one with higher values of the parameters a , b , c and lower value of the parameter d is recommended.

The above fact must be stated in terms of system parameters K_1 , K_2 , C_1 , and C_2 to convey the physical significance. System parameters K_1 , K_2 , C_1 , and C_2 are given in terms of nondimensional parameters a , b , c , and d in Appendix D. Also, as shown in Appendix D, the fact that it is advantageous to have the highest value for the nondimensional parameters a , b , c , and the lowest value for the nondimensional parameter d , can be restated in terms of system parameters as follows: within the range of parameters considered, it is advantageous to choose a padding material with the highest effective spring constant and the lowest effective damping coefficient for impact protection. The above conclusion is valid over the range of spring constants, K , varying from 5×10^6 N/m to 30×10^6 N/m and damping coefficients, C , varying from 5150 Ns/m to 7600 Ns/m. The application of the model beyond this range may be invalid because the model used involves the deformation of rate-independent material properties.

The values of the four visco-elastic parameters used to represent the response of the padding material to impact depend upon the material properties like the modulus of elasticity, porosity and also on the process parameters like

the geometry of the padding material and boundary conditions.

From the study of Figures 9 through 12, it is observed that the normalized force ϕ as a function of normalized time τ^* curves cross over. Physically the above fact can be explained as follows. The higher the peak force, the higher is the energy dissipating activity, and the faster is the decay of force. Hence the curve with higher peak force, which is decaying at a faster rate, crosses over the latter curve with lower peak force, which is decaying at a slower rate.

Considering two materials having identical static properties, the one which propagates strain at a higher rate has higher energy absorption capabilities because a greater amount of material can participate in energy absorption. The shock propagation rate of the material can be found from the dynamic stress-strain diagram. The greater the slope of the diagram, the faster will be the rate of propagation of strain and greater will be the energy absorption. From the study of Figures 13 through 16 which give the dynamic stress-strain response of padding materials as function of parameters a , b , c and d , respectively, it can be seen that the variation of these parameters does not change the slope of the curves. That is, the four-parameter, visco-elastic model is unable to account for the strain rate propagation in the material. This may be due to the fact that the four visco-elastic parameters do not directly account for the geometry of the material except for the

thickness.

From the study of Figures 13 through 16 it can be seen that the peak force increases with decreasing maximum padding deformation and that, depending on the choice of the visco-elastic padding parameters, separation between impacting object and padding occurs late in the deformation process. This is a limitation on the present model which stems from the imposition of displacement continuity $\Sigma x_1 = 0$. Important, however, is that this separation, associated with tension in padding, occurs in the model when the impact is completed and also the strain energy associated with tension is very small when compared with the total impact energy. Further refinements of the model are required to eliminate this interfacial tension, and the restrictions imposed on the choice of the four padding parameters by the requirement that the maximum padding deformation must be less than the original thickness.

CHAPTER VI

CONCLUSIONS AND RECOMMENDATIONS

In the context of the analysis presented, the following conclusions can be drawn.

1. The permissible range of rate independent material parameters is restricted by the limit of maximum possible padding deformation.

2. The analysis presented in this thesis permits one to assess the effects of visco-elastic support properties and impact parameters on the energy absorption through parameter variation.

3. In impact protection applications, the padding materials are required to absorb the maximum possible energy and reduce peak force encountered during the first few milliseconds of impact. To satisfy this criterion, within the range of material parameters considered, it is advantageous to choose a material with the highest values for the nondimensional parameters a , b , c , and the lowest value for the nondimensional parameter d . Interpreting this in physical terms, it is advantageous to select a material with the highest effective spring constant and the lowest effective damping coefficient.

Recommendations

1. Further refinements of the model are required, (a) to describe correctly the separation of the impactor from the padding system during rebound, and (b) to eliminate the restrictions imposed on the choice of the four padding parameters, by the requirement that the maximum padding deformation must be less than the original thickness, i.e., to include the strain rate dependence of properties.

2. The analysis presented above shows that the response of the padding material to impact can be represented by a four parameter viscoelastic model. This model has one relaxation time corresponding to $\tau_k = C_1/K_1$ of the Kelvin element. Single fibers and fibrous assemblies have a series of relaxation times represented by a series of Kelvin elements. In a further analysis, the possibility of representing the padding materials by a series of Kelvin elements, instead of a single Kelvin element should be explored.

3. In any future exhaustive analysis, an attempt should be made to incorporate the complete geometry of the padding material in the model.

4. With slight modifications, the above analysis can also be used to describe the response of the padding materials to arbitrarily prescribed forcing functions, such as produced in periodically occurring support motions. These results are applicable to packaging problems.

Finally, further research is needed for optimization

of padding systems, both through analytical techniques in conjunction with the modeling analysis and through experimental research carried out with the aid of a suitable impact test apparatus.

APPENDICES

APPENDIX A

AN EQUIVALENT MODEL TO ONE SHOWN IN FIGURE 1

The response of the padding material to impact which was described by a four parameter model (Figure 1) can be described with equal precision by another model which has similar parameters, but which are arranged in a different manner. The equivalent model has two Maxwellian elements coupled in parallel to one another.

Parameters K_1 , K_2 , C_1 , C_2 of the model in Figure 1 and K_3 , K_4 , C_3 , C_4 of the equivalent model are connected by the equations [13]:

$$K_2 = K_3 + K_4, \quad (\text{A.1})$$

$$K_1 = \frac{K_3 K_4 (C_3 + C_4)^2 (K_3 + K_4)}{(C_3 K_4 - C_4 K_3)^2}, \quad (\text{A.2})$$

$$C_1 = \frac{C_3 C_4 (K_3 + K_4)^2 (C_3 + C_4)}{(C_3 K_4 - C_4 K_3)^2}, \quad (\text{A.3})$$

$$C_2 = C_3 + C_4, \quad (\text{A.4})$$

and

$$K_3 = \frac{1}{2\beta} \left[K_2^\alpha + K_2^\beta - \frac{K_2^2}{C_1} - \frac{K_2^2}{C_2} \right], \quad (\text{A.5})$$

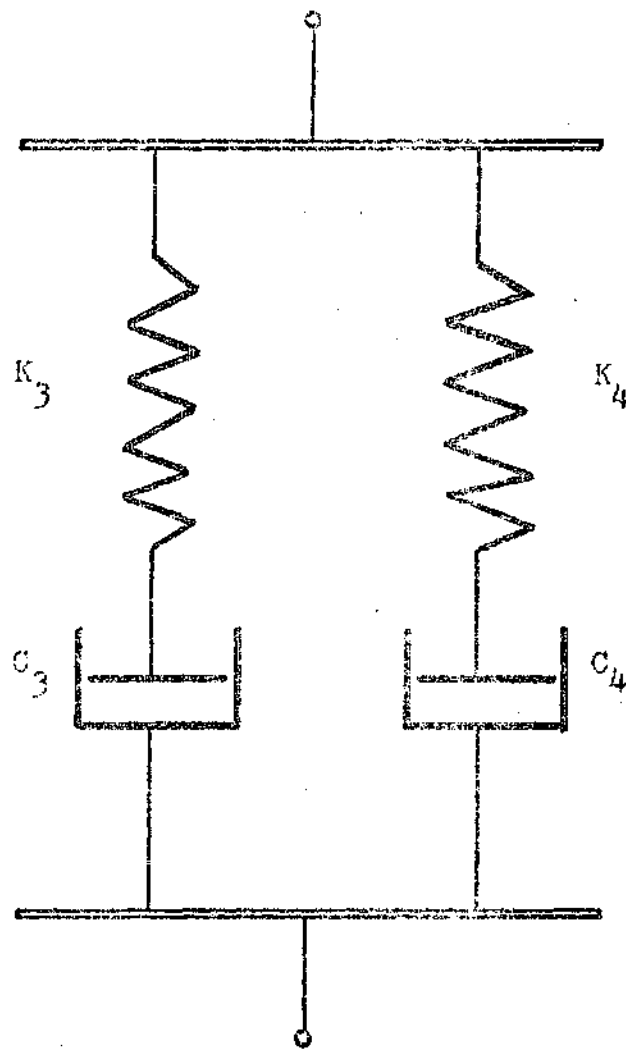


Figure 21. An Equivalent Model
(To one shown in Figure 1)

$$K_4 = -\frac{1}{2\beta} \left[K_2 \alpha - K_2 \beta - \frac{K_2^2}{C_1} - \frac{K_2^2}{C_2} \right], \quad (\text{A.6})$$

$$C_3 = \frac{1}{2\beta} \left[K_2 \alpha + K_2 \beta - \frac{K_2^2}{C_1} - \frac{K_2^2}{C_2} \right] \left[\frac{1}{\alpha - \beta} \right], \quad (\text{A.7})$$

$$C_4 = -\frac{1}{2\beta} \left[K_2 \alpha - K_2 \beta - \frac{K_2^2}{C_1} - \frac{K_2^2}{C_2} \right] \left[\frac{1}{\alpha + \beta} \right], \quad (\text{A.8})$$

where

$$\alpha = \left[\frac{K_2}{2C_2} + \frac{K_2}{2C_1} + \frac{K_2}{2C_1} \right] \quad (\text{A.9})$$

and

$$\beta = \alpha^2 - \frac{K_1 K_2}{C_1 C_2}. \quad (\text{A.10})$$

Although models 1 and 2 are mathematically equivalent, model 1 was selected because it has certain advantages from an interpretative stand point. Each term in the first model has a direct physical significance and is connected with one particular mechanism of response to stress. On the other hand, in the second model the elements have only an indirect physical significance. Also when the response of the padding materials to time invariant force is considered, the adaptation of the first model reduces the mathematical effort involved.

APPENDIX B

DERIVATION OF EQUATION 2.11

Call equation 2.4

$$y = x_1 - x_2 = \epsilon_1 + \epsilon_2 + \epsilon_3, \quad (\text{B.1})$$

where

- y is the total padding deformation,
- ϵ_1 = deformation in the Kelvin element,
- ϵ_2 = deformation in the spring with constant K_2 ,
- ϵ_3 = deformation in the dashpot with constant C_2 .

From equation B.1,

$$k_1 y = k_1 \epsilon_1 + k_1 \epsilon_2 + k_1 \epsilon_3, \quad (\text{B.2})$$

and

$$C_1 \frac{dy}{dt} = C_1 \frac{d\epsilon_1}{dt} + C_1 \frac{d\epsilon_2}{dt} + C_1 \frac{d\epsilon_3}{dt}. \quad (\text{B.3})$$

Adding equations B.2 and B.3 one obtains

$$k_1 y + C_1 \frac{dy}{dt} = k_1 \epsilon_1 + C_1 \frac{d\epsilon_1}{dt} + k_1 \epsilon_2 + k_1 \epsilon_3 + C_1 \frac{d\epsilon_2}{dt} + C_1 \frac{d\epsilon_3}{dt}. \quad (\text{B.4})$$

Since the forces in series elements are the same,

$$F = K_2 \epsilon_2 ,$$

and thus,

$$\frac{d\epsilon_2}{dt} = \frac{1}{K_2} \frac{dF}{dt} .$$

Also,

$$F = C_2 \frac{d\epsilon_3}{dt} ,$$

yielding,

$$\epsilon_3 = \int_0^t \frac{F}{C_2} dt .$$

Further,

$$F = K_1 \epsilon_1 + C_1 \frac{d\epsilon_1}{dt} .$$

Substituting the values of ϵ_1 , $\frac{d\epsilon_1}{dt}$, ϵ_2 , $\frac{d\epsilon_2}{dt}$, ϵ_3 and $\frac{d\epsilon_3}{dt}$ in equation B.4

$$\begin{aligned}
 K_1 y + C_1 \frac{dy}{dt} &= F + \frac{K_1}{K_2} F + K_1 \int_0^t \frac{F}{C_2} dt + \frac{C_1}{K_2} \frac{dF}{dt} + C_1 \frac{F}{C_2} \\
 &= \left(1 + \frac{K_1}{K_2} + \frac{C_1}{C_2}\right) F + \frac{C_1}{K_2} \frac{dF}{dt} + K_1 \int_0^t \frac{F}{C_2} dt .
 \end{aligned}
 \tag{B.5}$$

Differentiating both sides with respect to time,

$$K_1 \dot{y} + C_1 \ddot{y} = \left(1 + \frac{K_1}{K_2} + \frac{C_1}{C_2}\right) \dot{F} + \frac{C_1}{K_2} \ddot{F} + \frac{K_1}{C_2} \dot{F} .
 \tag{B.6}$$

Rearranging,

$$\ddot{F} = -\frac{K_1 K_2}{C_1 C_2} F - \left[1 + \frac{K_1}{K_2} + \frac{C_1}{C_2}\right] \frac{K_2}{C_1} \dot{F} + \frac{K_1 K_2}{C_1} \dot{y} + K_2 \ddot{y} .
 \tag{B.7}$$

APPENDIX C

DETAILS OF NORMALIZATION

The equations of motion and the initial conditions are normalized to derive the modeling rules, equations 2.10, 2.11, and 2.12 are the three differential equations for the dependent variables x_1 , x_2 and F_2 . The details of normalization of these equations (in that order) are presented below.

From equations 2.15 through 2.19,

$$x = \zeta \delta, \quad (C.1)$$

$$x_2 = \eta \delta, \quad (C.2)$$

$$y = \xi \delta \quad (C.3)$$

$$F = \frac{m_1 v_o^2}{\delta} \phi \quad (C.4)$$

and

$$\tau^* = \frac{\tau v_o}{\delta} \rightarrow \frac{d^n}{d\tau^n} = \left(\frac{v_o}{\delta}\right)^n \frac{d^n}{d(\tau^*)^n} \quad (C.5)$$

In equation 2.10,

$$\ddot{x}_1 = \frac{m_1 g}{m_1 + m_2} - \frac{F}{m_1 + m_2},$$

substituting the values of \ddot{x}_1 and F_2 from equations C.1, C.4 and C.5, and non-dimensionalizing, we get

$$\ddot{\zeta} = \frac{m_1}{m_1 + m_2} (g/\delta) \left(\frac{\delta}{v_0}\right)^2 - \frac{m_1}{m_1 + m_2} \left(\frac{\delta}{v_0}\right)^2 \left(\frac{v_0}{\delta}\right)^2. \quad (C.6)$$

Or

$$\ddot{\zeta} = A - B\phi, \quad (C.7)$$

where,

$$B = \frac{m_1}{m_1 + m_2} \approx 1 \quad (C.8)$$

and

$$A = \frac{Bg\delta}{v_0^2}. \quad (C.9)$$

In equation 2.11,

$$\ddot{x}_2 = \frac{F_2}{m_3} - \frac{k_3}{m_3} x_2 - \frac{C_3 \dot{x}_2}{m_3},$$

substituting the values of x_2 , \dot{x}_2 , \ddot{x}_2 and F_2 from equations C.2, C.4, and C.5, and non-dimensionalizing, we get

$$\ddot{\eta} = \frac{m_1}{m_3} \left(\frac{\delta}{v_0}\right)^2 \left(\frac{v_0}{\delta}\right)^2 \phi - \frac{k_3}{m_3} \left(\frac{\delta}{v_0}\right)^2 \eta - \frac{C_3}{m_3} \left(\frac{\delta}{v_0}\right) \dot{\eta}, \quad (\text{C.10})$$

Or

$$\ddot{\eta} = -\alpha\dot{\eta} - \beta\eta + \gamma\phi, \quad (\text{C.11})$$

where,

$$\alpha = \frac{C_3}{m_3} \left[\frac{\delta}{v_0}\right], \quad (\text{C.12})$$

$$\beta = \frac{k_3}{m_3} \left[\frac{\delta}{v_0}\right]^2 \quad (\text{C.13})$$

and

$$\gamma = \frac{m_1}{m_3}. \quad (\text{C.14})$$

In equation 2.12,

$$\ddot{F}_2 = \frac{-k_1 k_2}{C_1 C_2} F_2 - \frac{k_2}{C_1} \left[1 + \frac{k_1}{k_2} + \frac{C_1}{C_2}\right] \dot{F}_2 + \frac{k_1 k_2}{C_1} \dot{y} + k_2 \ddot{y}$$

substituting the values of F_2 , \dot{F}_2 , \ddot{F}_2 , \dot{y} and \ddot{y} from the equations C.3, C.4, and C.5, and nondimensionalizing, we get,

$$\frac{m_1 v_0^2}{\delta} \left(\frac{v_0}{\delta}\right)^2 \ddot{\phi} = \frac{-k_1 k_2}{C_1 C_2} \frac{m_1 v_0^2}{\delta} - \frac{k_2}{C_1} \left(1 + \frac{k_1}{k_2} + \frac{C_1}{C_2}\right) \frac{m_1 v_0^2}{\delta} \left(\frac{v_0}{\delta}\right) \dot{\phi} + \frac{k_1 k_2}{C_1} \left(\frac{v_0}{\delta}\right) \delta \dot{\xi} + k_2 \delta \left(\frac{v_0}{\delta}\right)^2 \ddot{\xi}. \quad (\text{C.15})$$

Rearranging,

$$\ddot{\phi} = -\frac{k_1 k_2}{C_1 C_2} \left(\frac{\delta}{v_0}\right)^2 \phi - \frac{k_2}{C_1} \left(1 + \frac{k_1}{k_2} + \frac{C_1}{C_2}\right) \left(\frac{v_0}{\delta}\right) \dot{\phi} + \frac{k_1 k_2}{C_1 m_1} \left(\frac{\delta}{v_0}\right)^3 \dot{\xi} + \frac{k_2}{m_1} \left(\frac{\delta}{v_0}\right)^2 \ddot{\xi} . \quad (\text{C.16})$$

Or

$$\ddot{\phi} = -a\dot{\phi} - b\phi + c\dot{\xi} + d\ddot{\xi} , \quad (\text{C.17})$$

where,

$$a = \frac{k_2 \delta}{C_1 v_0} \left[1 + \frac{k_1}{k_2} + \frac{C_1}{C_2}\right] , \quad (\text{C.18})$$

$$b = \frac{k_1 k_2}{C_1 C_2} \left[\frac{\delta}{v_0}\right]^2 , \quad (\text{C.19})$$

$$c = \frac{k_2}{m_1} \left[\frac{\delta}{v_0}\right]^2 \quad (\text{C.20})$$

and

$$d = \frac{k_1 k_2}{C_1 m_1} \left[\frac{\delta}{v_0}\right]^3 . \quad (\text{C.21})$$

Initial Conditions:

The normalization of the initial conditions given in equations 2.2, 2.13, and 2.14 is given below.

In equation 2.13,

$$\dot{x}_1(0) = V_0,$$

substituting the value of $\dot{x}_1(0)$ from equations C.1 and C.5, and non-dimensionalizing, we get

$$\delta \left(\frac{V_0}{\delta} \right) \dot{\zeta}(0) = V_0 . \quad (C.22)$$

Or

$$\dot{\zeta}(0) = 1 . \quad (C.23)$$

Also,

$$\dot{x}_1(0) - \dot{x}_2(0) = V_0 , \quad (C.24)$$

substituting the values of $\dot{x}_1(0)$ from equations C.1 and C.5, and non-dimensionalizing, we get

$$\delta \left(\frac{V_0}{\delta} \right) \dot{\zeta}(0) - 0 = V_0 . \quad (C.25)$$

Or

$$\dot{\xi} = \dot{\zeta} = 1 . \quad (C.26)$$

Assuming the rate of variation of force at the moment of impact to be equal to $K_2 V_0$,

$$\dot{F}_2 = K_2 V_0 , \quad (C.27)$$

substituting the value of \dot{F} from equations C.4 and C.5, and non-dimensionalizing, we get

$$\frac{m_1 v_0^2}{\delta} \left(\frac{v_0}{\delta} \right) \dot{\phi} = K_2 V_0 . \quad (C.28)$$

Or

$$\phi = \frac{K_2 \delta^2}{m_1 v_0^2} = \frac{P_3}{P_4} . \quad (C.29)$$

APPENDIX D

SYSTEM PARAMETERS IN TERMS OF NONDIMENSIONAL PARAMETERS

In order to convey physical significance and to express in terms of quantities which can be experimentally determined, it is necessary to show the results obtained in terms of nondimensional parameters a, b, c and d in terms of system parameters K_1, K_2, C_1 and C_2 . To achieve the above objective, the system parameters are expressed in terms of nondimensional parameters.

From equations 2.29 through 2.32 and equations 2.37 through 2.40,

$$a = \left(\frac{K_2}{C_1} + \frac{K_2}{C_2} + \frac{K_1}{C_1} \right) J, \quad (D.1)$$

$$b = \frac{K_1 K_2}{C_1 C_2} J^2, \quad (D.2)$$

$$c = \frac{K_2}{m_1} J^2 \quad (D.3)$$

and,

$$d = \frac{K_1 K_2}{C_1 m} J^3 \quad (D.4)$$

where,

$$J = \delta/V_0 .$$

From equation D.3,

$$K_2 = \frac{cm_1}{J^2} . \quad (D.5)$$

Dividing equation D.4 by equation D.3 and rearranging,

$$C_2 = \frac{d}{c} \left(\frac{m_1}{J} \right) . \quad (D.6)$$

In equation D.4 substituting the value of K_2 from equation D.5 and rearranging,

$$\frac{K_1}{C_1} = \frac{d}{cJ} . \quad (D.7)$$

Dividing equation D.5 by equation D.6,

$$\frac{K_2}{C_2} = \frac{c^2}{dJ} . \quad (D.8)$$

Substituting the values K_2 , K_1/C_1 and K_2/C_2 from equations D.5, D.7 and D.8 in equation D.1 and rearranging,

$$C_1 = \frac{cm_1}{(a - \frac{c^2}{d} - \frac{d}{c})J} \quad (D.9)$$

From equations D.7 and D.9,

$$K_1 = \frac{dm_1}{(a - c^2/d - d/c)J^2} \quad (D.10)$$

In Chapter V it was noted that it is advantageous to choose a material with highest values for the nondimensional parameters a, b, c , and the lowest value for the nondimensional parameter d for impact protection.

From equation D.5 it can be observed that the value of the spring constant K_2 increases with the increasing value of the nondimensional parameter c . Also from equation D.6 it can be noted that the value of the damping coefficient C_2 decreases with increasing value of the parameter c and decreasing value of the parameter d . The behavior of the damping coefficient C_1 and the spring constant K_1 is less apparent from equations D.9 and D.10. But from equation D.1 it can be seen that increasing the value of the parameter a amounts to increasing the spring constant K_1 and to decreasing the damping coefficient C_1 . Hence, it is observed that the selection of a padding material with highest values for the spring constants K_1, K_2 and lowest values for the damping coefficients C_1, C_2 is desirable. That is, the selection of

a material with the highest effective spring constant and the lowest effective damping coefficient is recommended.

BIBLIOGRAPHY

1. CIDITVA Bulletin No. 17 (Technical Aspects of Road Safety), 1964, pages 3-5.
2. Gadd, C. W. et al., "Tolerance and Properties of Superficial Tissue in Situ," Proceedings of Fourteenth Stapp Car Crash Conference, Society of Automotive Engineers, Inc., New York, 1970.
3. Brinn, J. et al., "Evaluation of Impact Test Accelerations: A Damage Index for the Head and Torso," Proceedings of Fourteenth Stapp Car Crash Conference, Society of Automotive Engineers, Inc., New York, 1970.
4. Freeston, W. D., et al., "The Stress-Strain Response of Yarns at High Rates of Loading," Journal of the Textile Institute, Volume 63, Number 5, May, 1972, pages 239-262.
5. Freeston, W. D. and Claus, W. D., "Strain Wave Reflections During Ballistic Impact of Fabric Panels," Textile Research Journal, (to be published).
6. Meinecke, E. A. et al., "Impact Analysis of Cellular Polymeric Materials," Journal of Elasto-Plastics, Volume 3, January, 1971, pages 19-27.
7. Coskren, R. J., Chu, C. C., and Morgan, H. M., WADD-Technical Report 60-511, parts 1-3, 1960-63.
8. Coskren, R. J. and Chu, C. C., AFML-TR-66-30, 1966.
9. Sebring, R. E., Freeston, W. D., Jr., Platt, M. M., and Coskren, R. J., AFML-TR-67-267, part III, 1967.
10. Wilde, A. E. et al., "Dynamic Response of a Constrained Fibrous System Subjected to Transverse Impact, Part I Transient Responses and Breaking Energies of Nylon Yarns," Army Materials and Mechanics Research Center, TR-70-32, 1970.
11. Nielson, L. E., Mechanical Properties of Polymers, Reinhold Publishing Corporation, 1967, pages 47-48.
12. Polakowski, N. H. and Ripling, E. J., Strength and Structure of Engineering Materials, Prentice Hall, Inc., 1966, pages 208-216.

13. Alfrey, T., Mechanical Behavior of High Polymers, Interscience Publishers, Inc., 1948, pages 125-126.
14. Jackson, A. S., Analog Computation, McGraw-Hill, New York, 1960.
15. Stephenson, R. E., Computer Simulation for Engineers, Harcourt Brace Javanovich, Inc., 1971.
16. Tse, F. S. et al., Mechanical Vibrations, Allyn and Bacon, Inc., Boston, 1966.
17. Systron-Donner Corporation, Handbook of Analog Computation.
18. Wulff, W., "Development of a Test for Impact Protection," Research proposal submitted to the National Bureau of Standards, United States Department of Commerce, in response to RFP No. 2-35927, June 1, 1972.
19. Modern Plastic Encyclopedia, Volume 50, No. 10A, 1973.